



저작자표시-비영리-변경금지 2.0 대한민국

이용자는 아래의 조건을 따르는 경우에 한하여 자유롭게

- 이 저작물을 복제, 배포, 전송, 전시, 공연 및 방송할 수 있습니다.

다음과 같은 조건을 따라야 합니다:



저작자표시. 귀하는 원저작자를 표시하여야 합니다.



비영리. 귀하는 이 저작물을 영리 목적으로 이용할 수 없습니다.



변경금지. 귀하는 이 저작물을 개작, 변형 또는 가공할 수 없습니다.

- 귀하는, 이 저작물의 재이용이나 배포의 경우, 이 저작물에 적용된 이용허락조건을 명확하게 나타내어야 합니다.
- 저작권자로부터 별도의 허가를 받으면 이러한 조건들은 적용되지 않습니다.

저작권법에 따른 이용자의 권리는 위의 내용에 의하여 영향을 받지 않습니다.

이것은 [이용허락규약\(Legal Code\)](#)을 이해하기 쉽게 요약한 것입니다.

[Disclaimer](#)

약학석사 학위논문

**Proliposomes for enhanced oral
bioavailability of BCS class II drugs:
valsartan and celecoxib**

향상된 경구 생체이용률을 위한 BCS class II

약물의 프로리포솜 적용: 발사르탄과

세레콕시브

2016 년 2 월

서울대학교 대학원

약학과 약제과학 전공

전 다 은

Abstract

Proliposomes for enhanced oral bioavailability of BCS class II drugs: valsartan and celecoxib

Daeun Jeon

Department of Pharmaceutics, College of Pharmacy

The Graduate School

Seoul National University

Purpose. The aim of this study was to develop a simple preparation method of proliposomes (PLs) with a high lipid content, and to characterize and evaluate the BCS class II drug-loaded PLs (valsartan-loaded PLs (VSTPLs) and celecoxib-loaded PLs (CXBPLs)) *in vitro* and *in vivo* for their suitability for oral delivery.

Methods. Rotary evaporator and freeze dryer were used to prepare PLs. Maximum lipid contents of PLs which can form liposomes after reconstitution were determined. After loading drugs, the solid state of PLs was also characterized by scanning electron microscopy (SEM), powder X-ray diffractometer (PXRD) and differential scanning calorimetry (DSC). PLs

were reconstituted with distilled water, and then were characterized by measuring the particle size, zeta potential, entrapment efficiency (EE), and drug content. Particle morphology of reconstituted liposomes was determined by transmission electron microscopy (TEM). *In vitro* dissolution and *in vivo* pharmacokinetics of PLs in rats were also evaluated.

Results. Phospholipid content of the PLs was increased up to 20% (w/w), thereby being able to enhance the drug loading content. Crystalline state of the drug was transformed to amorphous state during the preparation of PLs. Particle size of reconstituted VST-loaded liposomes and CXB-loaded liposomes were 369 ± 31 nm and 537 ± 10 nm with the zeta potential of -57.4 ± 0.4 mV and -64.2 ± 0.3 mV, respectively. The EE values of VST and CXB were $77.5 \pm 2.8\%$ and $84.7 \pm 1.2\%$ for VST-loaded liposomes and CXB-loaded liposomes, respectively. The rate and extent of dissolution of drugs from the PLs were higher than those of crude drug powder in various pHs. In pharmacokinetic studies after oral administration in rats, drugs in PLs showed higher C_{\max} values and 1.82-fold and 1.73-fold higher AUC values for VSTPLs and CXBPLs, respectively, than those from the drug powder. Shorter T_{\max} was shown in CXBPLs than that of crude drug powder.

Conclusions. The preparation method of PLs developed in this study has the following advantages compared with conventional preparation methods: (a) the preparation method is simple and could be easily scaled up, (b) the solvent system used has no toxicity concern, (c) the PLs have a higher lipid content, which can enhance the incorporation of poorly water-soluble drugs, (d) the rapid formation of liposomes in aqueous media and the amorphous state of the drug in PLs can increase solubility and dissolution rate, thereby increase oral

bioavailability of the drug.

Keywords: Proliposomes, Valsartan, Celecoxib, Dissolution rate, Oral
bioavailability

Student Number: 2014-21972

Table of Contents

Abstract	i
List of Tables	vi
List of Figures	vii
List of Tables and Figures of Supplementary Information	viii
1. Introduction	1
2. Materials and methods	4
2.1 Materials.....	4
2.2 Preparation of proliposomes (PLs).....	4
2.3 Characterization of PLs.....	5
2.3.1 Solid state characterization	5
2.3.1.1 Field emission scanning electron microscopy (FESEM).....	5
2.3.1.2 Differential scanning calorimetry (DSC).....	5
2.3.1.3 Powder X-ray diffractometry (PXRD).....	6
2.3.2 Characterization of liposomes.....	6
2.3.2.1 Transmission electron microscopy (TEM).....	6
2.3.2.2 Particle size and zeta potential.....	6
2.3.2.3 Determination of drug content and entrapment efficiency (EE).....	7
2.4 <i>In vitro</i> dissolution studies	8
2.4.1 <i>In vitro</i> dissolution studies of VSTPLs	8
2.4.2 <i>In vitro</i> dissolution studies of CXBPLs	9
2.5 <i>In vivo</i> pharmacokinetic studies	10
2.5.1 <i>In vivo</i> pharmacokinetic studies of VSTPLs.....	10

2.5.2 <i>In vivo</i> pharmacokinetic studies of CXBPLs	11
2.5.3 Pharmacokinetic parameters	13
2.6 Statistical Analysis	13
3. Result and discussion	14
3.1. Preparation of proliposomes (PLs).....	14
3.2 Characterization of PLs	15
3.2.1 Solid state characterization	15
3.2.2 Characterization of liposomes.....	17
3.3 <i>In vitro</i> dissolution studies	17
3.3.1 <i>In vitro</i> dissolution studies of VSTPLs	17
3.3.2 <i>In vitro</i> dissolution studies of CXBPLs	18
3.4 <i>In vivo</i> pharmacokinetic studies	19
3.4.1 <i>In vivo</i> pharmacokinetic studies of VSTPLs.....	19
3.4.2 <i>In vivo</i> pharmacokinetic studies of CXBPLs	20
4. Conclusions	22
5. References.....	23
Supplementary Information	40
국문초록	49

List of Tables

Table 1. Composition of the developed proliposomal formulations.....	28
Table 2. Characterization of the developed proliposomal formulations	29
Table 3. Pharmacokinetic parameters of valsartan (VST) after oral administration of crude VST powder and VSTPLs at a dose of 3 mg/kg in rats	30
Table 4. Pharmacokinetic parameters of celecoxib (CXB) after oral administration of crude CXB powder, Celebrex, and CXBPLs at a dose of 2 mg/kg in rats.....	31

List of Figures

Figure 1. Schematic illustration of the preparation method of PLs.....	32
Figure 2. SEM images of sorbitol, VST, CXB, Celebrex, VSTPLs, and CXBPLs. The lengths of the scale bars are 1 μm	33
Figure 3. Characterization of VSTPLs and CXBPLs. (a) DSC thermograms and (b) X-ray diffraction patterns.....	34
Figure 4. Size distribution and TEM images of the liposomes after reconstitution of blank PLs, VSTPLs, and CXBPLs. The length of the scale bars are 0.5 μm	35
Figure 5. <i>In vitro</i> dissolution profiles of crude VST powder and VSTPLs at pH 1.2, 4.0, 6.8, and DDW. Data are presented as the mean \pm SD ($n = 3$)...	36
Figure 6. <i>In vitro</i> dissolution profiles of crude CXB powder, Celebrex, and CXBPLs at pH 1.2, 4.0, 6.8, and 12.0. Data are presented as the mean \pm SD ($n = 3$).....	37
Figure 7. Plasma concentration vs. time profiles of VST after a single oral administration of crude VST powder and VSTPLs at a dose of 3 mg/kg. The values are presented on a (a) semilogarithmic plot and (b) linear scale. Data are presented as the mean \pm SD ($n \geq 3$).....	38
Figure 8. Plasma concentration vs. time profiles of CXB after a single oral administration of crude CXB powder, Celebrex, and CXBPLs at a dose of 2 mg/kg. The values are presented on a (a) semilogarithmic plot and (b) linear scale (inset: expanded view form time 0 to 250 min). Data are presented as the mean \pm SD ($n \geq 3$).....	39

List of Tables and Figures of Supplementary Information

Figure S1. Images of PLs prepared (a) without solvent evaporation step and (b) with the 25% (w/w) of lipid content.....	40
Table S1. Composition and evaporation temperature of simvastatin-loaded proliposomes (SVPLs).....	41
Table S2. Characterization of SVPLs.....	42
Figure S2. The effect of the amount of CXB in CXBPLs on the (a) mean diameter and (b) EE values after reconstitution	44
Table S3. Solubility of VST in various media.....	45
Table S4. Solubility of CXB in various media.....	46
Figure S3. TEM images of VST-loaded liposomes in various dissolution media (pH 1.2, 4.0, 6.8, and DDW). The length of the scale bar is shown in Figure	48

1. Introduction

More than 40% of new chemical entities (NCE) have poor aqueous solubility [1]. Since aqueous solubility is essential for drugs to enter the systemic circulation and show medicinal effect, the poor solubility of drugs is an issue to solve in drug development [2]. Drugs with poor water solubility (biopharmaceutical system (BCS) class II and IV) could suffer from low bioavailability [1, 3]. Therefore, several attempts have been made to increase solubility of drug to improve oral bioavailability such as solid dispersion [4-6], emulsion [2], spherical agglomeration [7], nanosuspension [8], nanoparticles [9], spray-drying [10], and liposomes [11].

Among these formulation strategies to increase the solubility of drugs, lipid-based drug delivery systems, such as liposomes, have been widely used for increasing solubility, improving dissolution, and enhancing oral bioavailability of drugs [2]. Liposomes are vesicular system composed of phospholipid, which could encapsulate lipophilic to hydrophilic compounds, small- to macro-molecules [12]. The absorption mechanisms of drug associated with liposomes in the gastrointestinal tract are: (a) liposomes could be absorbed by endocytosis, (b) liposome-vesicles could adsorb to mucosal membrane and fuse with the cell membrane, (c) drugs released from liposomes could enter cell *via* micropinocytosis, (d) liposomes could alter the colloidal environment of intestinal milieu by forming mixed micelles and micelles with physiological bile salts [13-15]. However, liposomes have stability problems such as susceptibility to hydrolysis and oxidation of lipid layer, vesicle

aggregation, fusion and sedimentation related to leakage of entrapped drugs [3, 12, 13].

To overcome the instability of liposomes, the concept of proliposomes (PLs) was adopted. PLs are dry, free flowing powder which could form more uniform-sized liposomes over conventional liposomes by hydration [3, 12]. Since PLs are dry formulation, they could prevent vesicle aggregation and fusion during storage [16]. Being available in dry powder form, further modification is easy (e.g. tableting or capsule filling after mixing with other pharmaceutical excipients) [12, 17]. Also, PLs showed enhanced dissolution and improved bioavailability of drugs [3, 18]. Various preparation methods of PLs were established using rotary evaporator [16, 19], spray dryer [13], fluidized bed [20], and supercritical anti-solvent technology [21]. These conventional methods are in need of specific equipment (e.g. spray dryer, fluidized bed granulator) and the procedures are complicated to control [12].

The aim of this present study were to (a) develop a simple method to prepare PLs (b) evaluate the resultant PLs incorporating BCS class II model drug: valsartan (VST) and celecoxib (CXB). VST is an orally active highly selective angiotensin II type 1 receptor antagonist used for the treatment of hypertension [22]. VST has relatively low bioavailability (~25%) caused by its poor aqueous solubility [2, 22]. CXB is a selective cyclooxygenase 2 (COX-2) inhibitor for treatment of arthritis and acute pain [4]. CXB has incomplete and highly variable oral bioavailability caused by its low water solubility (~ 5 µg/mL) [4]. VST and CXB are categorized as BCS class II drugs which have high permeability but low solubility [3, 4]. Applying proliposomal formulations to BCS class II drugs, the solubility and dissolution of drugs

could be increased, thereby enhancing oral bioavailability of drugs.

2. Materials and methods

2.1. Materials

VST was purchased from Tecoland (Irvine, CA). CXB and Celebrex were kindly gifted by Hanlim Pharm. Co., Ltd. (Seoul, Korea). Soy phosphatidyl choline (SPC) was a gift from PHYTOS (Gyeonggi, Korea). Anhydrous ethanol of 99.9% purity was purchased from Daejung (Gyeonggi, Korea). Poloxamer 188 was purchased from BASF (Ludwigshafen, Germany), sorbitol sodium dodecyl sulfate (SDS) was purchased from Sigma–Aldrich (St. Louis, MO). All other reagents were of analytical grade.

2.2. Preparation of proliposomes (PLs)

VST-loaded proliposomes (VSTPLs) and CXB-loaded proliposomes (CXBPL) were prepared by rotary evaporator and freeze-dryer (Figure 1). Briefly, SPC (800 mg), poloxamer 188 (40 mg), and VST (160 mg) or CXB (100 mg) were dissolved in ethanol (8.75 ml). The mixture was vortex-mixed and sonicated to obtain a clear yellow solution. Sorbitol (3160 mg) was dissolved in double-deionized water (DDW) (3.75 ml). The two solutions were mixed in a round-bottom flask with gentle stirring for 30 min. The mixture was then evaporated under vacuum for 10 min at 40°C using a rotary evaporator. After removing ethanol, the resulting solution was immediately lyophilized over 24 h. The obtained PLs were ground using a pestle and mortar.

The powder which passed through the sieve of 25 mesh size but could not pass through 100 mesh size was collected. The pale-yellow powder was stored at -4°C for further experiments. The blank PLs were prepared following the same methods without drugs.

2.3 Characterization of PLs

2.3.1 Solid state characterization

2.3.1.1 Field emission scanning electron microscopy (FESEM)

The particle morphology of sorbitol, Celebrex, VST, CXB, VSTPLs, and CXBPLs were characterized by FESEM. The micrographs were recorded on a JSM-6700F from JEOL (Japan). For FESEM measurement, the samples were placed on carbon tape and sputter-coated with a thin layer of platinum for 120 sec prior to measurements. The coated samples were randomly scanned and photomicrographs were taken with FESEM.

2.3.1.2 Differential scanning calorimetry (DSC)

DSC experiments were conducted using DSC-Q1000 (TA Instrument, UK). Accurately weighed samples were scanned from 0°C to 200°C with a scan speed of 10°C/min.

2.3.1.3 Powder X-ray diffractometry (PXRD)

PXRD was used to assess the degree of crystallinity of drugs and other raw materials before and after preparing PLs. The analysis was carried out using a D8 ADVANCE with DAVINCI (BRUKER, German) Cu α_1 radiation (1.5418 Å). An acceleration voltage and current of 40 kV and 40 mA were used, respectively. Samples were scanned between 3 ° and 50 ° with a step size of 0.02 ° and a scan speed of 0.5 sec/step.

2.3.2 Characterization of liposomes

2.3.2.1 Transmission electron microscopy (TEM)

Reconstituted liposomal dispersion was made by putting 10 mg of PLs into 1 mL of DDW and agitating with hand for 5 min. For TEM measurement, a drop of dispersion was placed onto a surface of a 200 mesh carbon-coated copper grid (Electron Microscopy Sciences, USA). The liposome particles settled on the grid were negatively stained with uranyl acetate. The excess DDW was removed with a filter paper and left to dry at room temperature. Then, the grid was loaded into TEM (JEM1010, Jeol, Japan) and investigated at 80 kV.

2.3.2.2 Particle size and zeta potential

The particle size and zeta potential of reconstituted liposomes were evaluated by electrophoretic light scattering spectrophotometer (ELS-Z,

Otsuka Electronics, Japan).

2.3.2.3 Determination of drug content and entrapment efficiency (EE)

To determine drug content of PLs, 10 mg of drug-loaded PLs were dissolved in 50% acetonitrile (ACN) with bath sonication. The drug concentration of the sample was determined by the HPLC method described below. The drug content was calculated from the following equation:

$$\text{Drug content (\%)} = \frac{\text{actual drug amount in proliosomes}}{\text{total weight of proliosomes}} \times 100$$

To determine EE after reconstitution with DDW, 10 mg/mL of drug-loaded PLs were made with gentle handshaking for 5 min and filtered through 0.45 μm syringe filter (Minisart RC15, Sartorius, Germany) to remove undissolved drug. An aliquot (100 μL) of filtered dispersion was diluted with 900 μL of ACN to break down liposomes and dissolve drugs which were entrapped into the liposomes. The concentration of drug of the samples was determined by following HPLC method. The drug entrapment efficiency (EE) was calculated from the following equation:

$$\text{EE (\%)} = \frac{\text{actual drug amount in liposomal dispersion after filtration}}{\text{theoretical drug amount in liposomal dispersion}} \times 100$$

To determine the VST concentration, reverse-phase HPLC was performed on a Waters e2695 system consisting of a 2475 multi λ fluorescence detector (Waters Corporation, USA). For the chromatographic separation of VST, a Phenomenex Gemini-NX analytical column (250 \times 4.6 mm, 5 μ m) was used with isocratic elution using ACN with 0.025% trifluoroacetic acid (TFA) / 5 mM phosphate buffer (pH 2.5) with 0.025% TFA (70:30, v/v) mixture as the mobile phase at a flow rate of 1.0 mL/min. The wavelength for detection was set at 234 nm and 378 nm for excitation and emission, respectively. All samples were appropriately diluted with the mobile phase prior to analysis.

To determine the CXB concentration, reverse-phase HPLC was performed on a Waters e1525 system consisting of a 2487 dual λ absorbance detector (Waters Corporation, USA). For the chromatographic separation of CXB, a Phenomenex Gemini-NX analytical column (250 \times 4.6 mm, 5 μ m) was used with isocratic elution using ACN with 0.1% triethylamine (TEA) / pH 9.0 10 mM phosphate buffer with 0.1 % TEA (70:30, v/v) mixture as the mobile phase at a flow rate of 1.0 mL/min. The wavelength for detection was set at 260 nm. All samples were appropriately diluted with the mobile phase prior to analysis.

2.4 *In vitro* dissolution studies

2.4.1 *In vitro* dissolution studies of VSTPLs

The dissolution of VSTPLs and crude VST powder were tested using a USP

type II (paddle) dissolution apparatus (Electrolab TDT-08L, India). DDW, pH 1.2, 4.0, and 6.8 buffer media were used as a different dissolution media at a temperature of $37.0 \pm 0.2^\circ\text{C}$ and a paddle speed of 50 rpm. Crude VST powder or VSTPLs (equivalent to 10 mg of VST) was encapsulated into hard capsules and the filled capsules were added to dissolution medium with sinker. The volume of dissolution medium was 500 mL for DDW, pH 4.0, and pH 6.8 buffer, and 1000 mL for pH 1.2 buffer to maintain the sink condition (Table S3). Aliquots of samples (5 mL) were withdrawn from the dissolution vessel at predetermined time intervals (5, 10, 20, 30, 45, 60, 90, and 120 min) and the same volume of fresh medium was added to maintain constant volume of dissolution medium. The withdrawn samples were passed through a $0.45\ \mu\text{m}$ syringe filter to remove undissolved VST. An aliquot of filtrate was properly diluted and analyzed by HPLC as described in 2.3.2.3 section.

2.4.2 *In vitro* dissolution studies of CXBPLs

The dissolution of CXBPLs, Celebrex, and crude CXB powder were tested using a USP type II (paddle) dissolution apparatus (Electrolab TDT-08L, India) at various pH (pH 1.2, 4.0, 6.8 and 12.0). Buffer media (500 mL) containing 0.4% (w/v) SDS were used (Table S4) at a temperature of $37 \pm 0.2^\circ\text{C}$ with paddle rotating at a speed of 50 rpm. Each formulation equivalent to 2 mg of CXB was encapsulated into hard capsules. The filled capsules were added to dissolution medium with sinker. Samples (1 mL) were withdrawn from the dissolution vessel at predetermined time intervals (15, 30, 45, 60, 90, and 120 min) and equal volume of fresh medium was replaced. Samples were filtered

through a 0.45 μ m syringe filter to remove undissolved CXB. The filtrate was properly diluted and analyzed by HPLC as described in 2.3.2.3 section.

2.5 *In vivo* pharmacokinetic studies

2.5.1 *In vivo* pharmacokinetic studies of VSTPLs

A pharmacokinetic study in Sprague-Dawley rats was designed to evaluate the VSTPL by comparison with the crude VST powder at a 3 mg/kg dose. The rats, weighing 235 \pm 5 g, were housed in compliance with good laboratory practice (GLP). The rats were fasted for at least 12 h prior to dosing but had free access to water. The rats were randomly divided into 2 treatment groups ($n \geq 3$). Each formulation was encapsulated into #9 hard gelatin capsule (Torpac, USA). Each capsule and following 1 mL of DDW was administered orally. After administration, 250 μ L of blood sample were obtained at predetermined time intervals (10, 20, 30, 45, 60, 90, 120, 240, and 480 min). The samples were immediately centrifuged at 4°C and 13,200 rpm for 2.5 min (5415R, Eppendorf centrifuge, Germany), and an aliquot (100 μ L) of supernatant plasma sample was collected and were stored below -20°C until further analysis.

To determine the VST concentration in rat plasma, pretreatment was conducted before analysis. The frozen samples were thawed at 37°C, and 100 μ L of plasma sample was mixed with 1 mL of internal standard solution (losartan, 5 μ g/mL in ACN) and vortex-mixed for 30 min. The sample was

then centrifuged at 13,200 rpm for 5 min. An aliquot (900 μ L) of the supernatant was separated and fluid was evaporated at 60°C under nitrogen gas purge. The residue was reconstituted with 50 μ L of 50% ACN, vortex-mixed for 10 min, centrifuged at 9,000 rpm for 30 sec, and 45 μ L of supernatant was collected for HPLC analysis.

A 10 μ L aliquot of prepared sample was injected into a Phenomenex Gemini-NX analytical column (250 \times 4.6 mm, 5 μ m) and eluted isocratically, using an 0.025% TFA in ACN / 0.025% TFA in 5mM phosphate buffer (pH 2.5) (60:40, v/v) mixture as a mobile phase, at a flow rate of 1.0 mL/min. The HPLC system used was Waters e2695 system consisting of a 2475 multi λ fluorescence detector (Waters Corporation, USA). The wavelength for VST detection was set at 234 nm and 378 nm for excitation and emission wavelengths, respectively.

2.5.2 *In vivo* pharmacokinetic studies of CXBPLs

A pharmacokinetic study in Sprague-Dawley rats was designed to evaluate the CXBPLs by comparison with Celebrex and the crude CXB powder at a 2 mg/kg dose. The rats, weighing 248 \pm 23 g, were housed in compliance with good laboratory practice (GLP). The rats were fasted for at least 12 h prior to dosing but had free access to water and were randomly divided into 3 treatment groups ($n \geq 3$). Each formulation equivalent to 2mg/kg of CXB was encapsulated into #9 hard gelatin capsule. Each capsule was administered orally at a single dose via an oral gavage. At predetermined time intervals (1, 5, 15, 30, 45, 60, 90, 120, 240, 360, 480 and 1440 min), 120 μ L of blood

sample were obtained and immediately centrifuged at 4°C and 13,200 rpm for 2.5 min (5415R, Eppendorf centrifuge, Germany) and an aliquot (50 µL) of supernatant plasma sample was collected and were stored below -20°C until further analysis.

Before analysis, the frozen samples were thawed at 37°C and spiked with 200 µL internal standard solution (VST, 100 ng/mL in ACN) and vortex-mixed for 5 min. The mixtures were centrifuged at 4°C and 13,200 rpm for 5 min, and 160 µL of supernatant was collected for LC/MS/MS analysis.

HPLC analysis was carried out using an Agilent Technologies 1260 Infinity HPLC system (Agilent Technologies, Inc.; Palo Alto, CA, USA), equipped with a G1312B binary pump, a G1367E autosampler, a G1316C thermostatted column compartment, and a G1330B thermostat. Chromatographic separation was achieved using a Agilent Poroshell 120 EC-C18 column (50 × 4.6 mm, 2.7 µm; Agilent Technologies) with a C18 guard column (4 mm × 2.0 mm; Phenomenex; CA, USA) with 5 µL of sample injection volume. The isocratic mobile phase is consisted of ACN and 5 mM ammonium formate buffer (95:5, v/v), at a flow rate of 0.4 mL/min. Mass analysis was performed at negative electrospray ionization (ESI) mode on an Agilent Technologies 6430 Triple Quad LC/MS system. The mass transitions from precursor to product ion, collision energy, and fragmentor voltage were m/z 380.2 → 316.2, 19 eV, and 170 V for CXB and m/z 434.1 → 350.0, 18 eV, and 140 V for VST, respectively. The retention times of CXB and VST were 1.8 and 1.5 min, respectively. MassHunter Workstation Software Quantitative Analysis (Version B.05.00; Agilent Technologies, Inc.) were used for data acquisition and processing.

2.5.3 Pharmacokinetic parameters

Plasma concentration of drug in rats were plotted against time, and the pharmacokinetic parameters were calculated using a non-compartmental model *via* WinNonlin software (version 3.1, Pharsight Corporation, USA). The area under the plasma concentration versus time curve from time zero to infinity (AUC) was obtained by the log-linear trapezoidal method, the peak plasma concentration of drug (C_{\max}), the time taken to reach the peak concentration (T_{\max}), and the elimination half-life ($t_{1/2}$) were obtained from the individual plasma concentration-time curve.

2.6 Statistical analysis

All experimental data were expressed as mean \pm standard deviation (S.D.). The statistical analysis was carried out using Student's *t*-test and one-way analysis of variance (ANOVA). The level of statistical significance was defined by $p < 0.05$. All experiments were conducted more than three times except for Figure S2.

3. Result and discussion

3.1. Preparation of PLs

VSTPLs, CBXPLs, and blank PLs were successfully prepared by using rotary evaporator and freeze dryer. Every raw material of PLs was dissolved into water-ethanol mixture. Ethanol was chosen as organic solvent because it is Class 3 residual solvent in '*USP 38 General Chapter <467> Residual Solvents*' which is regarded as less toxic and have low risk to human health.

This method has several strong points than conventional preparation method: (a) it has few process parameters than conventional preparation method including spray drying method, fluidized bed method, and super critical anti-solvent method, (b) the phospholipid content of the PLs could be increased.

Solvent evaporation process was introduced to remove only ethanol in the mixture and make aqueous solution. Heterogeneous proliposomal formulation was obtained when water-ethanol mixture went through lyophilization, because each solvent has its different sublimation temperature (Figure S1a). Low temperature (40°C) of solvent evaporation process attribute to consistent reproducibility of PLs (Table S2). Therefore, solvent evaporation is significant step to yield homogeneous proliposomal formulation. Lyophilization was adopted to remove remaining DDW in the formulation.

Sorbitol is widely used water soluble matrix in preparing proliposomal formulation [16, 23]. The high dissolution rate of porous sorbitol could result in rapid formation of spherical liposomes after reconstitution than other water

soluble matrices [23]. Poloxamer 188 was added to increase the stability of reconstituted liposomes [24]. To increase the amount of reconstituted drug-loaded liposomes in unit weight of the formulation, a high lipid to matrix ratio of PLs is desirable. By this method, the lipid content could be increased up to 20% (w/w). When the lipid content was increased up to 25% (w/w), the formulation had sticky property which was hard to modify further (e.g. grinding, capsule filling) (Figure S1b). Finally, the weight ratio of blank PLs was set at sorbitol/SPC/poloxamer 188 = 79/20/1. Drugs were added to the blank PLs formulation based on the preliminary study to set the amount of drugs added (Figure S2). The final composition of VSTPLs, CXBPLs, and blank PLs were shown in Table 1.

3.2 Characterization of PLs

3.2.1 Solid state characterization

The surface morphology of sorbitol, drugs, and PLs was evaluated by FESEM, as shown in Figure 2. Sorbitol showed porous structure [23]. VST had a rectangular crystalline structure [6], and CXB showed needle-shaped crystalline [25]. However, the characteristic structure of the drugs and sorbitol was disappeared after preparing into PLs.

The thermal behaviors of the drugs, excipients, and prepared PLs were shown in Figure 3a. A sharp endothermic peak was shown at around 103°C for VST, which was corresponded its melting temperature [1]. The DSC curve

for CXB showed an endothermic peak at around 160°C which is related to its melting temperature [26]. The characteristic endothermic peak of CXB was also shown in the DSC curve of Celebrex [10], indicating the crystalline state of CXB in Celebrex. Sorbitol and poloxamer 188 had their own endothermal peak which are similar to those reported in the previous reports [4, 27]. However, all those characteristic peaks were absent in thermograms of PLs, which illustrates that the crystalline drugs have changed into amorphous form during the preparation of PLs.

For further determination of the crystallinity of drugs in the formulation, the PXRD analysis was conducted and the diffractograms were shown in Figure 3b. As expected from DSC results, drugs and other excipients had their own characteristic peaks [4, 6, 26, 28], but the PLs showed a series of broad peaks. The characteristic peaks of drugs were absent in PXRD spectra of VSTPLs and CXBPLs in comparison with those of blank PLs. This indicates that the drugs entrapped in PLs were in an amorphous state, which agreed well with the DSC results.

Taken together, the drugs have changed from crystalline state to amorphous state during the preparation of PLs. The amorphous form of drugs could provide increased solubility and higher dissolution rate which might result in better bioavailability due to the higher free energy of the amorphous drug [1, 5, 29]. This was further illustrated by the *in vitro* dissolution tests and *in vivo* pharmacokinetic studies. The amorphous state of drugs in PLs maintained for at least 15 months and 5 months of low temperature (~ -20°C) storage period for VSTPLs and CXBPLs, respectively (Figure 3).

3.2.2 Characterization of liposomes

By adding DDW and manual agitation of PLs, about 370 nm and 540 nm of liposomes from VSTPLs and CXBPLs, respectively, were made (Table 2). The successful reconstitution to spherical liposomal suspension from PLs was confirmed by TEM observation (Figure 4). The prepared liposomes showed about -60 mV zeta potential values (Table 2). The negative zeta potential would suggest non-aggregated physical stability of reconstituted liposomal suspension [30, 31]. The EE of reconstituted liposomes was about 78% and 85% for VSTPLs and CXBPLs, respectively (Table 2).

3.3 *In vitro* dissolution studies

3.3.1 *In vitro* dissolution studies of VSTPLs

The dissolution profile of VST from VSTPLs and crude VST powder in various pH are depicted in Figure 5. The dissolution tests were carried out at various dissolution media (pH 1.2, 4.0, 6.8 and DDW). Each dissolution medium maintained the sink condition during the experiments (Table S3). The dissolved drug of crude VST powder were below 50% in all dissolution media, excluding at pH 6.8 because of the pH-dependent solubility of VST due to its weak acidity [1, 32]. However, VST dissolved from VSTPLs was increased compared to that of crude VST powder in all media. The increased dissolution of VST from VSTPLs might be due to the increased solubility of the

amorphous state of VST in the VSTPLs, as evidenced by the DSC and PXRD results, or VSTPLs formed VST-loaded liposomal dispersion by contacting dissolution medium, as consistent with the TEM results (Figure S3). Moreover, the improved dissolution at low pH might be helpful for enhanced absorption since the low bioavailability of VST is resulted by poor solubility of VST in acidic environment of the gastrointestinal tract [22].

3.3.2 *In vitro* dissolution studies of CXBPLs

The dissolution profiles of CXB from crude CXB powder, Celebrex, and CXBPLs in various pH are illustrated in Figure 6. The dissolution test were conducted at various dissolution media (pH 1.2, 4.0, 6.8 and 12.0). Each dissolution medium maintained the sink condition by adding 0.4% (w/v) SDS in all dissolution media (Table S4). The dissolved CXB from crude CXB powder was less than 30% in all dissolution media, except at pH 12.0 due to its weak acidity ($pK_a \approx 11.1$) [33]. The dissolution rate of Celebrex increased as the pH of dissolution medium increased. This might be due to the SDS in Celebrex formulation, which attribute the increased solubility of CXB, and croscarmellose sodium, which is used as a disintegrant. However, at pH 1.2, the dissolution rate of Celebrex was similar to that of crude CXB powder, which might be due to the lack of swelling property of croscarmellose sodium at low pH [34]. Remarkable dissolution enhancement was observed in CXBPLs at all dissolution medium. The dissolved CXB from CXBPLs showed more than 50% within 30 min and 100% in 120 min at all dissolution medium. The increased dissolution of CXB from CXBPLs might be due to (a)

the conversion to amorphous form from crystalline state of CXB in the CXBPLs during preparation (b) the CXB-loaded liposomes were formed quickly from CXBPLs by adding dissolution medium. Since CXB is a BCS class II drug which has poor drug absorption due to its poor dissolution property [8], the improved dissolution rate of CXBPLs would be helpful for enhanced oral bioavailability of CXB.

3.4 *In vivo* pharmacokinetic studies

3.4.1 *In vivo* pharmacokinetic studies of VSTPLs

The *in vivo* pharmacokinetics after oral administration of crude VST powder and VSTPLs were determined in rats. The plasma concentration versus time profiles were illustrated and pharmacokinetic parameters were listed in Figure 7 and Table 3. The VSTPL-treated group exhibited 1.88-fold and 1.82-fold higher C_{\max} and oral absorption (AUC), respectively, compared to those of crude VST powder-treated group ($p < 0.05$). The higher plasma concentration and systemic exposure of VST in VSTPL-treated group might be due to the increased dissolution rate in acidic pH, which are corresponded to *in vitro* dissolution results, together with other mechanisms proposed in the previous reports such as mixed-micelle formation with endogenous bile acids [14, 35]. The $t_{1/2}$ values of two groups were about the same (data not shown).

3.4.2 *In vivo* pharmacokinetic studies of CXBPLs

The *in vivo* pharmacokinetic study was carried on crude CXB powder, Celebrex, and CXBPLs in rats. Each formulation was administered orally and the plasma concentration of CXB was analyzed. The plasma CXB concentration versus time curve and pharmacokinetic parameters were shown in Figure 8 and Table 4. As expected in the *in vitro* dissolution tests, the systemic exposure (AUC) of CXBPL-treated group was significantly increased by 1.73-fold in comparison with the crude CXB powder-treated group ($p < 0.05$). The increased oral absorption might be due to various possible mechanisms such as mixed-micelle formation with endogenous bile acids in the gastrointestinal tract [14, 35], or might be due to increased dissolution rate by forming liposomal suspension in the gastrointestinal fluid and increased solubility of amorphous CXB of CXBPLs. The Celebrex-treated group exhibited significantly increased AUC (1.67-fold) compared to crude CXB-treated group ($p < 0.05$), as well. The increase of oral absorption of Celebrex might be attributed from the excipients such as SDS and disintegrants which might have been helpful for improving dissolution rate of CXB. However, the rank order of T_{max} from fastest to slowest and C_{max} from highest to lowest was as follows: CXBPLs > Celebrex > crude CXB powder. CXB can be absorbed throughout the gastrointestinal tract [36]. The T_{max} is related to *in vitro* dissolution rate of each formulation at physiologically relevant pH media (pH 1.2, 4.0, and 6.8). The rapid and high extent of dissolution of CXB in physiological pH might contribute to shorter T_{max} and higher C_{max} . There were no significant differences in $t_{1/2}$ values among three

groups (data not shown).

4. Conclusion

BCS class II drugs-loaded proliposomes with 20% (w/w) of lipid content were successfully prepared with simpler preparation method than convention methods. Solvent evaporation at low temperature (40°C) and lyophilization were used to remove solvent and yielded homogeneous formulation. The crystalline state of drugs has changed to amorphous form by preparing proliposomal formulation, which attributed to increased dissolution rate of drug-loaded PLs. The PLs rapidly formed liposomal suspension by adding water or dissolution medium, which also attributed to improved dissolution rate. Since the oral bioavailability of BCS class II drugs is limited to their poor dissolution, formulation which increase drug dissolution could improve oral absorption of BCS class II drugs. The enhanced oral bioavailability of drug-loaded PLs compared with crude drug powder was confirmed in rats. Taken together, the developed proliposomes offers a new approach to improve the oral absorption of BCS class II drugs like VST and CXB.

5. References

1. Ma, Q., et al., *Uniform nano-sized valsartan for dissolution and bioavailability enhancement: influence of particle size and crystalline state*. International Journal of Pharmaceutics, 2013. **441**(1-2): p. 75-81.
2. Baek, I.H., et al., *Oral absorption of a valsartan-loaded spray-dried emulsion based on hydroxypropylmethyl cellulose*. International Journal of Biological Macromolecules, 2014. **69**: p. 222-8.
3. Yanamandra, S., et al., *Proliposomes as a drug delivery system to decrease the hepatic first-pass metabolism: case study using a model drug*. European Journal of Pharmaceutical Sciences, 2014. **64**: p. 26-36.
4. Homayouni, A., et al., *Preparation and characterization of celecoxib solid dispersions; comparison of poloxamer-188 and PVP-K30 as carriers*. Iranian Journal of Basic Medical Sciences, 2014. **17**(5): p. 322-31.
5. Mosquera-Giraldo, L.I., Trasi, N.S., and Taylor, L.S., *Impact of surfactants on the crystal growth of amorphous celecoxib*. International Journal of Pharmaceutics, 2014. **461**(1-2): p. 251-7.
6. Yan, Y.D., et al., *Novel valsartan-loaded solid dispersion with enhanced bioavailability and no crystalline changes*. International Journal of Pharmaceutics, 2012. **422**(1-2): p. 202-10.
7. Gupta, V.R., et al., *Spherical crystals of celecoxib to improve solubility, dissolution rate and micromeritic properties*. Acta Pharmaceutica, 2007. **57**(2): p. 173-84.

8. Dolenc, A., et al., *Advantages of celecoxib nanosuspension formulation and transformation into tablets*. International Journal of Pharmaceutics, 2009. **376**(1–2): p. 204-12.
9. Liu, Y., et al., *Mechanism of dissolution enhancement and bioavailability of poorly water soluble celecoxib by preparing stable amorphous nanoparticles*. Journal of Pharmacy and Pharmaceutical Sciences, 2010. **13**(4): p. 589-606.
10. Lee, J., et al., *Enhanced dissolution rate of celecoxib using PVP and/or HPMC-based solid dispersions prepared by spray drying method*. Journal of Pharmaceutical Investigation, 2013. **43**(3): p. 205-13.
11. Dong, J., et al., *Intra-articular delivery of liposomal celecoxib–hyaluronate combination for the treatment of osteoarthritis in rabbit model*. International Journal of Pharmaceutics, 2013. **441**(1–2): p. 285-90.
12. Shaji, J. and Bhatia, V., *Proliposomes: a brief overview of novel delivery system*. International Journal of Pharma and Bio Sciences, 2013. **4**(1): p. 150-60.
13. Zheng, B., et al., *Proliposomes containing a bile salt for oral delivery of Ginkgo biloba extract: Formulation optimization, characterization, oral bioavailability and tissue distribution in rats*. European Journal of Pharmaceutical Sciences, 2015. **77**: p. 254-64.
14. Porter, C.J., Trevaskis, N.L., and Charman, W.N., *Lipids and lipid-based formulations: optimizing the oral delivery of lipophilic drugs*. Nature Review Drug Discovery, 2007. **6**(3): p. 231-48.
15. Torchilin, V.P., *Recent advances with liposomes as pharmaceutical*

- carriers*. Nature Review Drug Discovery, 2005. **4**(2): p. 145-60.
16. Jahn, A., et al., *AAPE proliposomes for topical atopic dermatitis treatment*. Journal of Microencapsulation, 2014. **31**(8): p. 768-73.
 17. Tantisripreecha, C., et al., *Development of delayed-release proliposomes tablets for oral protein drug delivery*. Drug Development and Industrial Pharmacy, 2012. **38**(6): p. 718-27.
 18. Yan-yu, X., et al., *Preparation of silymarin proliposome: A new way to increase oral bioavailability of silymarin in beagle dogs*. International Journal of Pharmaceutics, 2006. **319**(1-2): p. 162-8.
 19. Elhissi, A.M.A. and Taylor, K.M.G., *Delivery of liposomes generated from proliposomes using air-jet, ultrasonic, and vibrating-mesh nebulisers*. Journal of Drug Delivery Science and Technology, 2005. **15**(4): p. 261-5.
 20. Gala, R.P., et al., *A comprehensive production method of self-cryoprotected nano-liposome powders*. International Journal of Pharmaceutics, 2015. **486**(1-2): p. 153-8.
 21. Liu, G., et al., *Preparation of 10-hydroxycamptothecin proliposomes by the supercritical CO₂ anti-solvent process*. Chemical Engineering Journal, 2014. **243**: p. 289-96.
 22. Kim, J.E., et al., *Pharmacokinetic properties and bioequivalence of 2 formulations of valsartan 160-mg tablets: A randomized, single-dose, 2-period crossover study in healthy Korean male volunteers*. Clinical Therapeutics, 2014. **36**(2): p. 273-9.
 23. Elhissi, A.M.A., et al., *A study of size, microscopic morphology, and dispersion mechanism of structures generated on hydration of*

- proliposomes*. Journal of Dispersion Science and Technology, 2012. **33**(8): p. 1121-6.
24. Wu, G., et al., *Interaction between Lipid Monolayers and Poloxamer 188: An X-Ray Reflectivity and Diffraction Study*. Biophysical Journal, 2005. **89**(5): p. 3159-73.
25. Bohr, A., et al., *Preparation of microspheres containing low solubility drug compound by electrohydrodynamic spraying*. International Journal of Pharmaceutics, 2011. **412**(1-2): p. 59-67.
26. Chavan, R.B., Modi, S.R., and Bansal, A.K., *Role of solid carriers in pharmaceutical performance of solid supersaturable SEDDS of celecoxib*. International Journal of Pharmaceutics, 2015. **495**(1): p. 374-84.
27. Mathlouthi, M., Benmessaoud, G., and Rogé, B., *Role of water in the polymorphic transitions of small carbohydrates*. Food Chemistry, 2012. **132**(4): p. 1630-7.
28. Kim, E.J., et al., *Preparation of a solid dispersion of felodipine using a solvent wetting method*. European Journal of Pharmaceutics and Biopharmaceutics, 2006. **64**(2): p. 200-5.
29. Zhao, P., et al., *Inclusion of celecoxib into fibrous ordered mesoporous carbon for enhanced oral bioavailability and reduced gastric irritancy*. European Journal of Pharmaceutical Sciences, 2012. **45**(5): p. 639-47.
30. Tayel, S.A., et al., *Duodenum-triggered delivery of pravastatin sodium via enteric surface-coated nanovesicular spanlastic dispersions: development, characterization and pharmacokinetic assessments*. International Journal of Pharmaceutics, 2015. **483**(1-2): p. 77-88.

31. Freitas, C. and Müller, R.H., *Effect of light and temperature on zeta potential and physical stability in solid lipid nanoparticle (SLN™) dispersions*. International Journal of Pharmaceutics, 1998. **168**(2): p. 221-9.
32. Flesch, G., Muller, P., and Lloyd, P., *Absolute bioavailability and pharmacokinetics of valsartan, an angiotensin II receptor antagonist, in man*. European Journal of Clinical Pharmacology, 1997. **52**(2): p. 115-20.
33. Chawla, G., et al., *Characterization of solid-state forms of celecoxib*. European Journal of Pharmaceutical Sciences, 2003. **20**(3): p. 305-17.
34. Zhao, N. and Augsburger, L.L., *The influence of swelling capacity of superdisintegrants in different pH media on the dissolution of hydrochlorothiazide from directly compressed tablets*. AAPS PharmSciTech, 2005. **6**(1): p. E120-6.
35. Hauss, D.J., *Oral lipid-based formulations*. Advanced Drug Delivery Reviews, 2007. **59**(7): p. 667-76.
36. Paulson, S.K., et al., *Pharmacokinetics of celecoxib after oral administration in dogs and humans: effect of food and site of absorption*. Journal of pharmacology and experimental therapeutics, 2001. **297**(2): p. 638-45.

Table 1

Composition of the developed proliposomal formulations.

Component	Blank PLs	VSTPLs	CXBPLs
SPC	20.0% (800 mg)	19.2% (800 mg)	19.5% (800 mg)
Sorbitol	79.0% (3160 mg)	76.0% (3160 mg)	77.1% (3160 mg)
Poloxamer 188	1.0% (40 mg)	1.0% (40 mg)	1.0% (40 mg)
VST	-	3.8% (160 mg)	-
CXB	-	-	2.4% (100 mg)
Total	100% (4000 mg)	100% (4160 mg)	100% (4100 mg)

Table 2

Characterization of the developed proliposomal formulations.

Formulation	Mean diameter (nm)	Polydispersity index	Zeta potential (mV)	Entrapment efficiency (%) ^a	Drug content (%) ^b
Blank PLs	365.6 ± 14.5	0.30 ± 0.02	-59.00 ± 0.09	-	-
VSTPLs	368.8 ± 30.7	0.29 ± 0.08	-57.42 ± 0.36	77.5 ± 2.8	3.71 ± 0.04
CXBPLs	537.1 ± 10.2	0.36 ± 0.01	-64.15 ± 0.26	84.7 ± 1.2	2.35 ± 0.09

$$^a\text{Entrapment efficiency (\%)} = \frac{\text{actual drug amount in liposomal dispersion after filtration}}{\text{theoretical drug amount in liposomal dispersion}} \times 100$$

$$^b\text{Drug content (\%)} = \frac{\text{actual drug amount in proliposomes}}{\text{total weight of proliposomes}} \times 100$$

Data are presented as mean ± SD ($n = 3$).

Table 3

Pharmacokinetic parameters of VST after oral administration of crude VST powder and VSTPLs at a dose of 3 mg/kg in rats.

Parameter	crude VST powder	VSTPLs
AUC ($\mu\text{g}\cdot\text{min}/\text{mL}$)	160 \pm 50	291 \pm 72*
C _{max} ($\mu\text{g}/\text{mL}$)	0.70 \pm 0.25	1.32 \pm 0.30*
T _{max} (min)	45 \pm 15	58 \pm 29
Relative bioavailability (%)	100	182

* $p < 0.05$, compared to crude VST powder group.

Data are presented as mean \pm SD ($n \geq 3$).

Table 4

Pharmacokinetic parameters of CXB after oral administration of crude CXB powder, Celebrex, and CXBPLs at a dose of 2 mg/kg in rats.

Parameter	crude CXB powder	Celebrex	CXBPLs
AUC (µg·min/mL)	464 ± 117	774 ± 165*	803 ± 139*
C _{max} (µg/mL)	0.56 ± 0.17	1.05 ± 0.44	1.12 ± 0.23*
T _{max} (min)	240 ± 0	165 ± 90	64 ± 19*
Relative bioavailability (%)	100	167	173

* $p < 0.05$, compared to crude CXB powder group.

Data are presented as mean ± SD ($n \geq 3$).

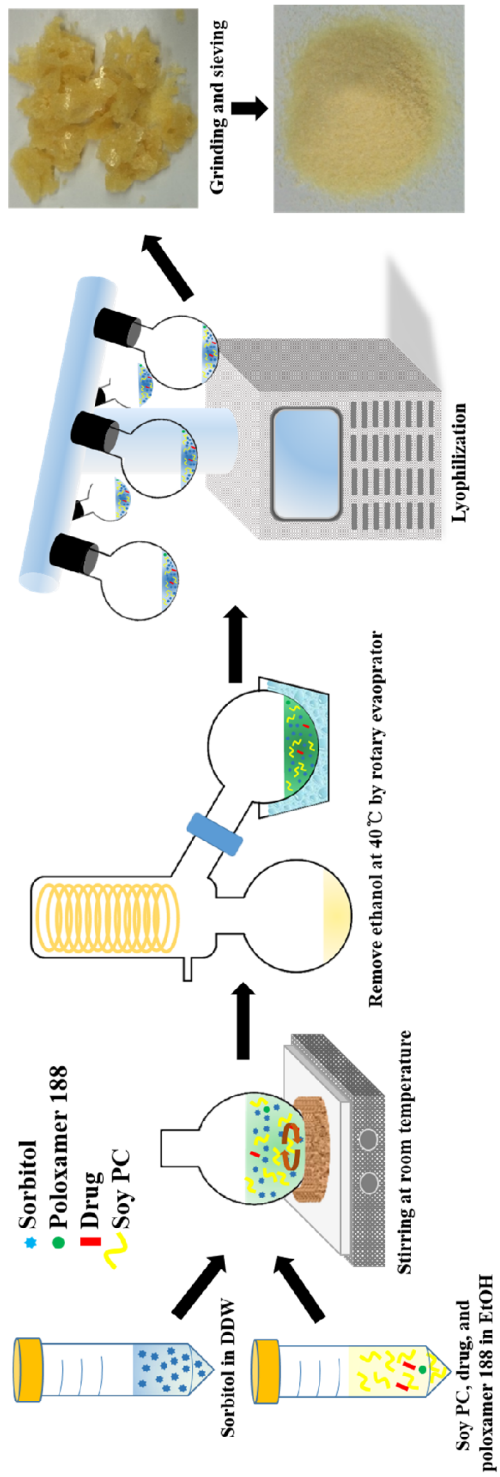


Figure 1. Schematic illustration of the preparation method of PLs.

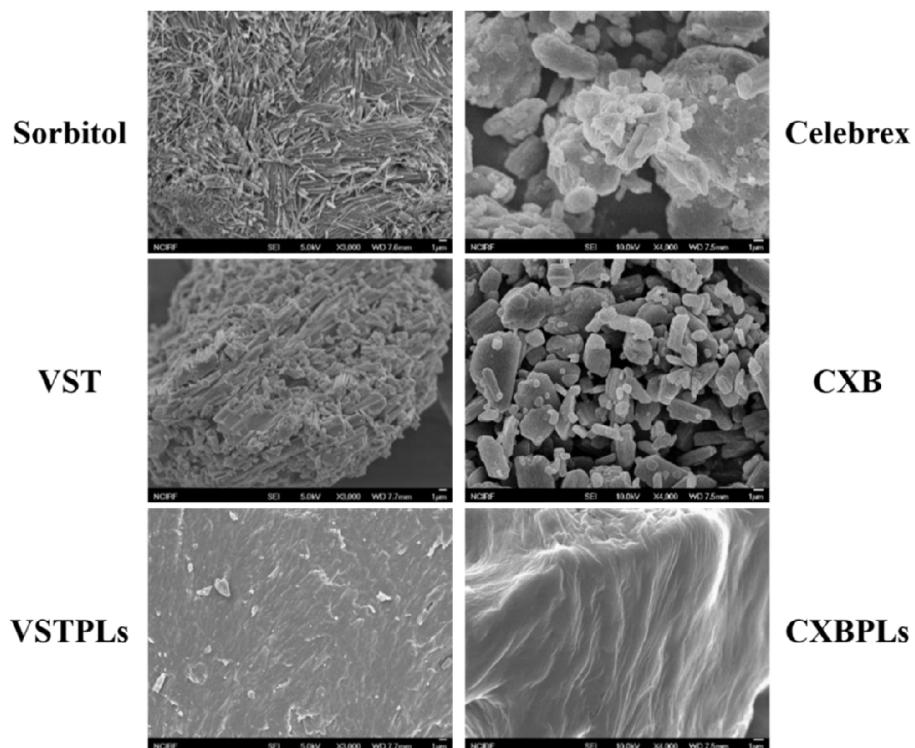


Figure 2. SEM images of sorbitol, VST, CXB, Celebrex, VSTPLs, and CXBPLs. The lengths of the scale bars are 1 μm .

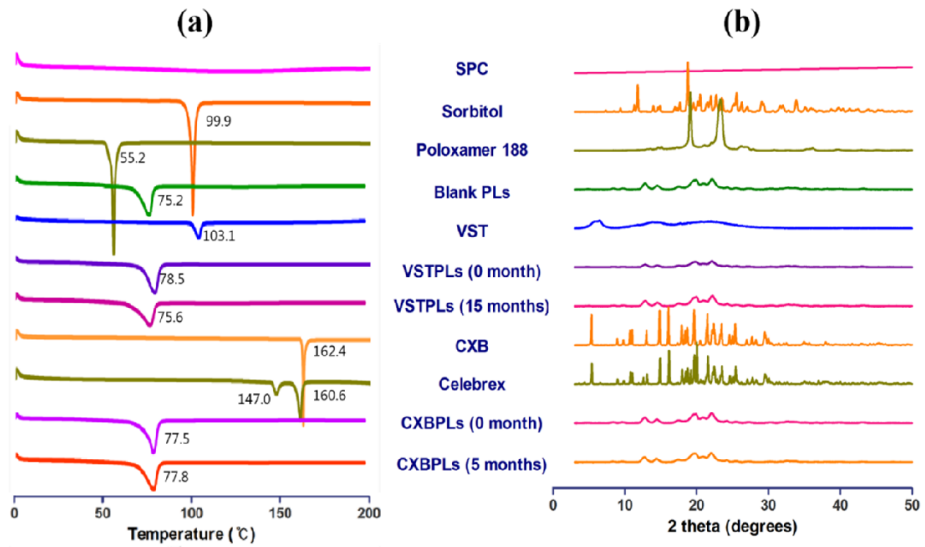


Figure 3. Characterization of VSTPLs and CXBPLs. (a) DSC thermograms and (b) X-ray diffraction patterns.

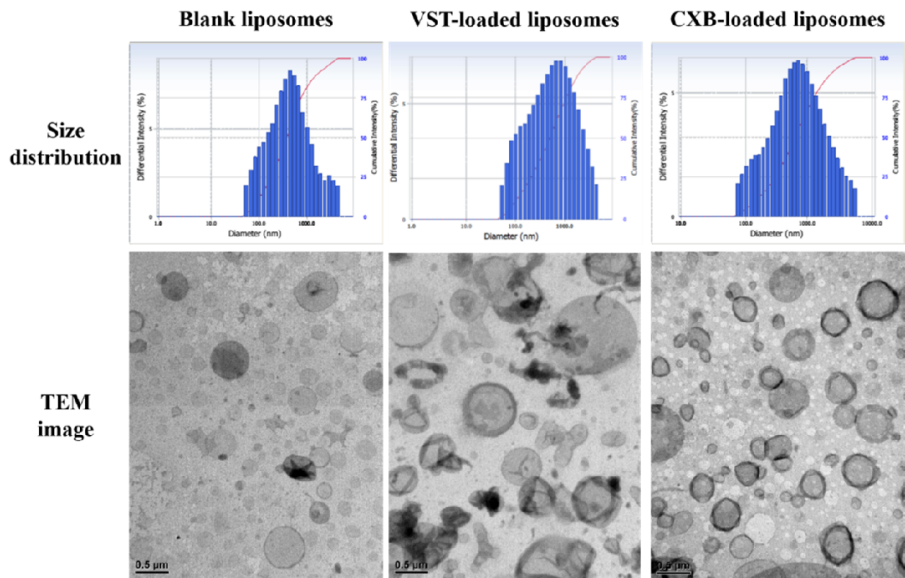


Figure 4. Size distribution and TEM images of the liposomes after reconstitution of blank PLs, VSTPLs, and CXBPLs. The length of the scale bars are 0.5 μm .

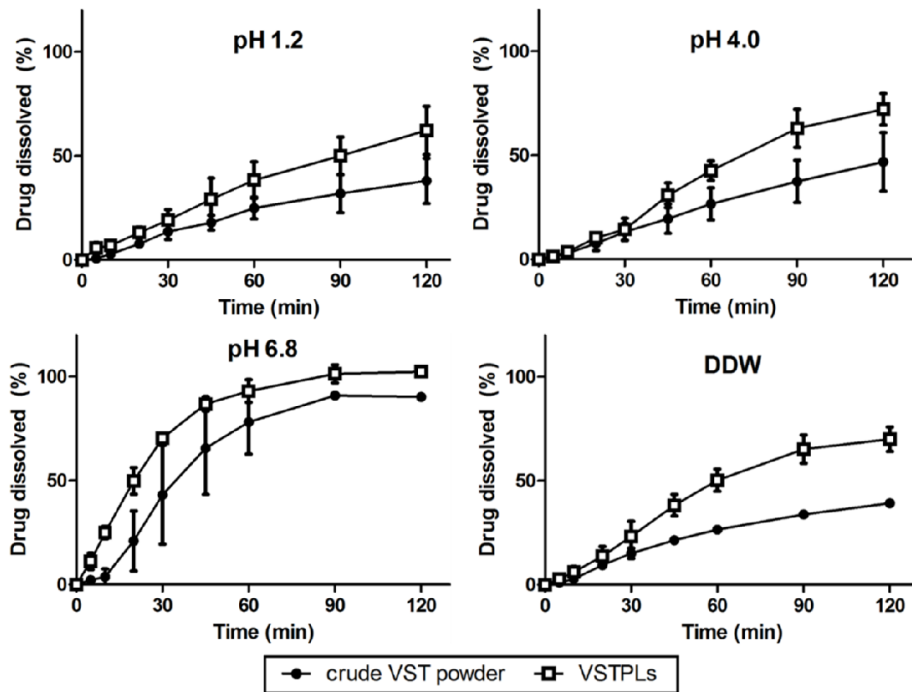


Figure 5. *In vitro* dissolution profiles of crude VST powder and VSTPLs at pH 1.2, 4.0, 6.8, and DDW. Data are presented as the mean \pm SD ($n = 3$).

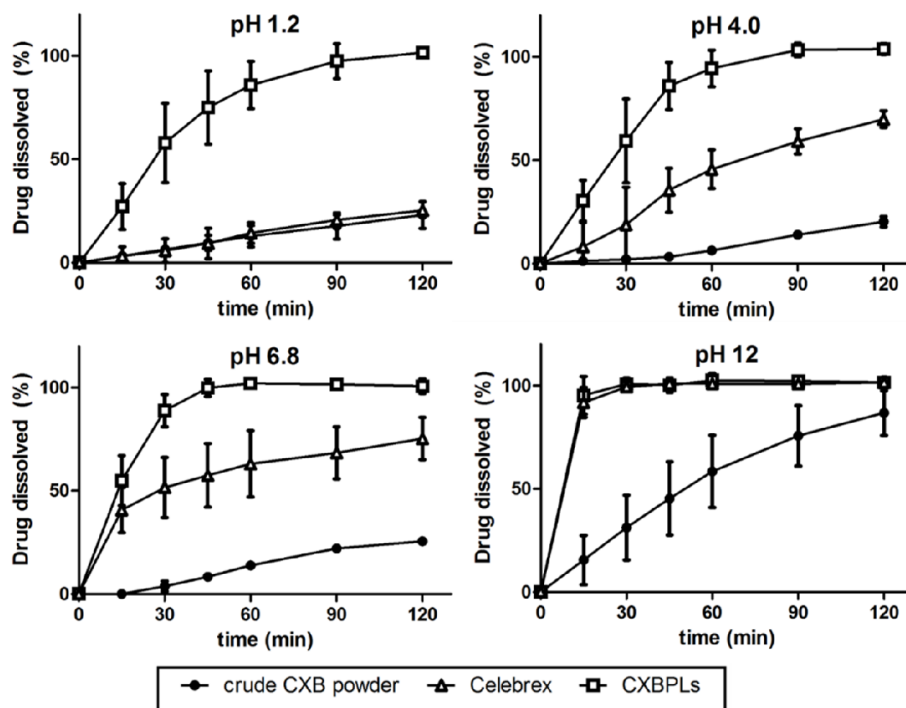


Figure 6. *In vitro* dissolution profiles of crude CXB powder, Celebrex, and CXBPLs at pH 1.2, 4.0, 6.8, and 12.0. Data are presented as the mean \pm SD ($n = 3$).

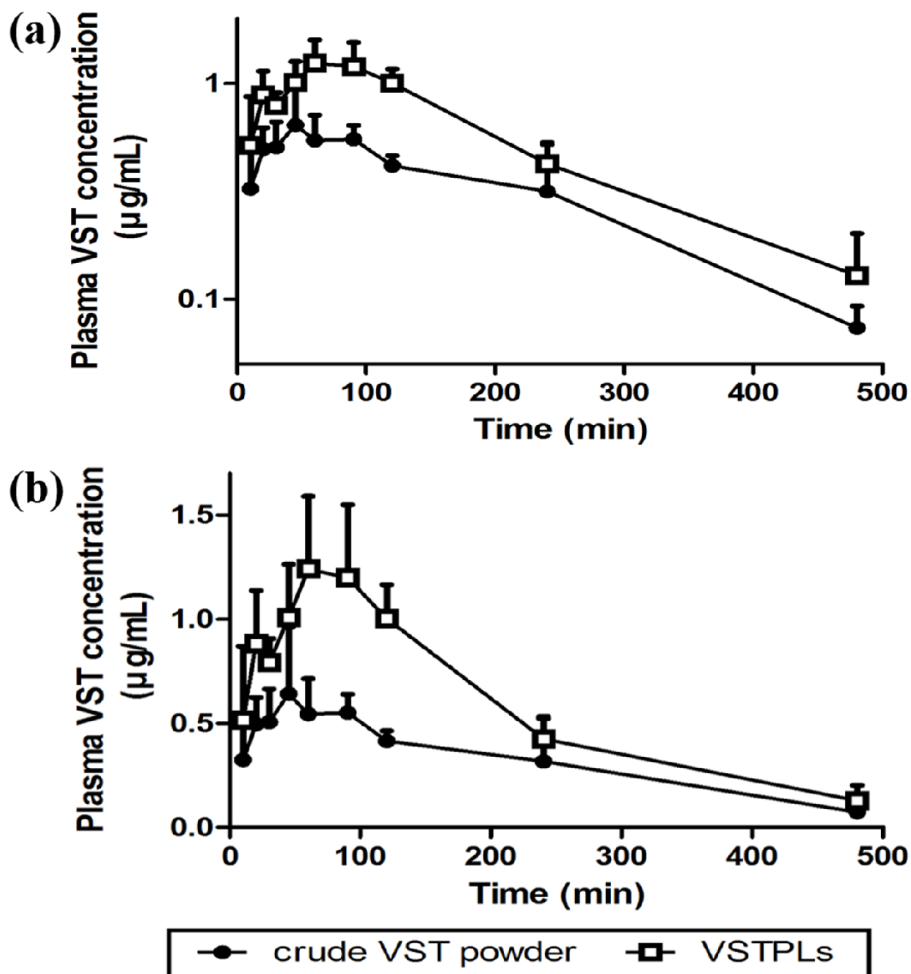


Figure 7. Plasma concentration vs. time profiles of VST after a single oral administration of crude VST powder and VSTPLs at a dose of 3 mg/kg. The values are presented on a (a) semilogarithmic plot and (b) linear scale. Data are presented as the mean \pm SD ($n \geq 3$).

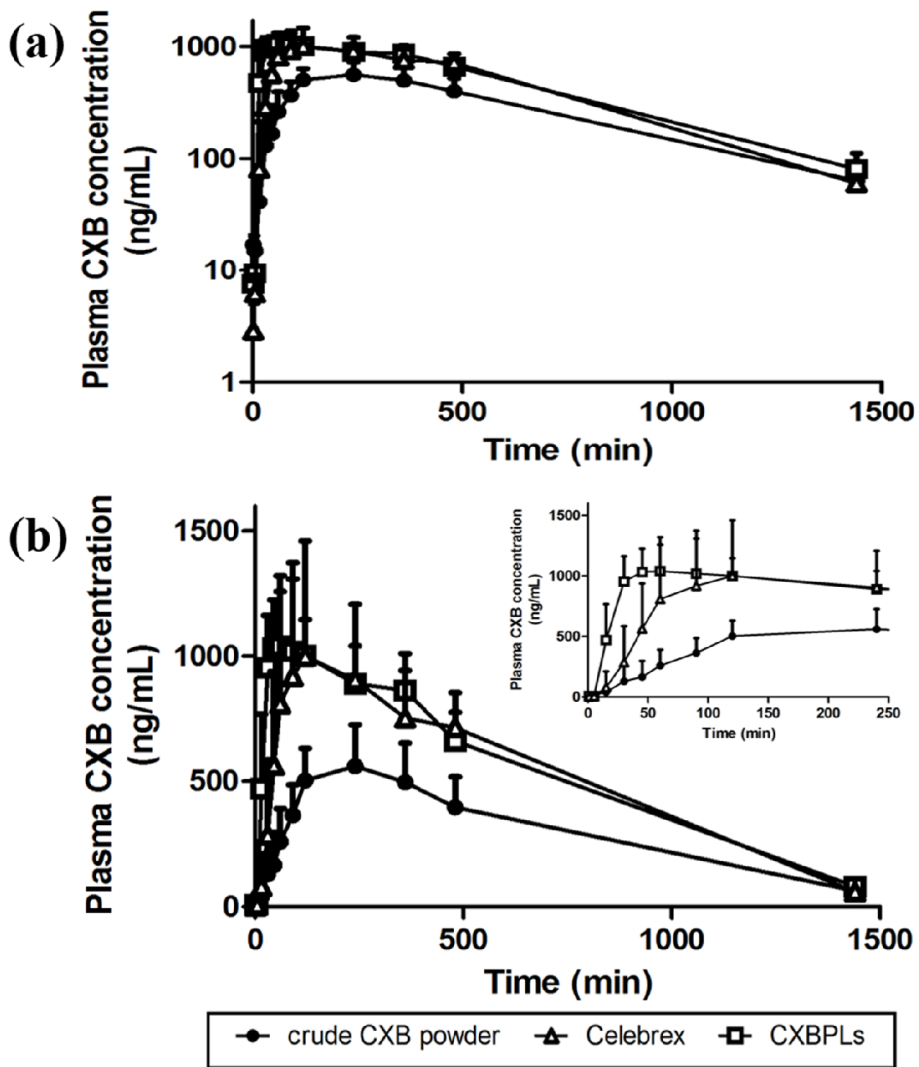


Figure 8. Plasma concentration vs. time profiles of CXB after a single oral administration of crude CXB powder, Celebrex, and CXBPLs at a dose of 2 mg/kg. The values are presented on a (a) semilogarithmic plot and (b) linear scale (inset: expanded view from time 0 to 250 min). Data are presented as the mean \pm SD ($n \geq 3$).

Supplementary Information

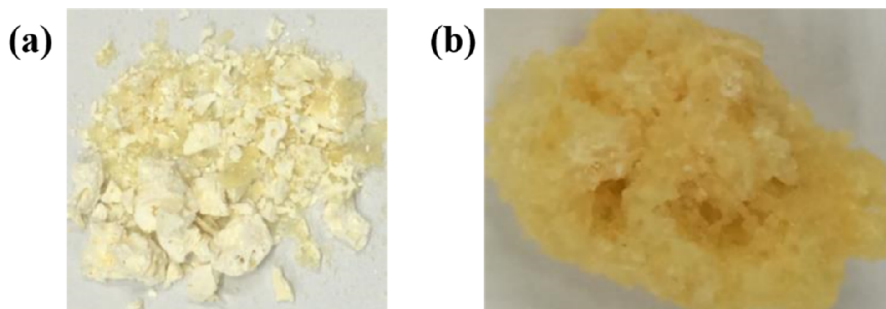


Figure S1. Images of PLs prepared (a) without solvent evaporation step and (b) with the 25% (w/w) of lipid content.

The solvent evaporation of ethanol before lyophilization is a critical step for homogeneous formulation. As mentioned in 3.1, without removal of ethanol, phase separation occur during lyophilization, since the tripe point of ethanol is too low to sublime by lyophilization. Ethanol in the solution melt down and withdraw ethanol-soluble material such as drugs and SPC from the solution during lyophilization process. This result in inhomogeneous formulation (Figure S1a).

To increase the amount of reconstituted liposomes in unit weight of the proliposomal formulation, a high lipid to matrix ratio of PLs is desirable. However, when the lipid content of PLs was over 20% (w/w), the stickiness of lipid remained in prepared PLs which made it difficult to modify further (Figure S1b).

Table S1

Composition and evaporation temperature of simvastatin-loaded proliposomes (SVPLs)

Component	SVPL - 60°C	SVPL - 40°C
SPC	19.2% (800 mg)	19.2% (800 mg)
Sorbitol	76.0% (3160 mg)	76.0% (3160 mg)
Poloxamer 188	1.0% (40 mg)	1.0% (40 mg)
SV	3.8% (160 mg)	3.8% (160 mg)
Evaporation temperature	60°C	40°C

Table S2

Characterization of SVPLs.

Formulation	Batch No.	Mean diameter (nm)	Polydispersity index	Entrapment efficiency (%)^a
SVPL - 60°C	1	598.8 ± 20.9	0.33 ± 0.05	73.0 ± 11.6
	2	925.6 ± 62.1	0.36 ± 0.02	33.0 ± 5.8
	3	768.7 ± 9.9	0.31 ± 0.00	51.7 ± 4.2
SVPL - 40°C	1	615.8 ± 11.7	0.35 ± 0.00	72.4 ± 1.8
	2	584.4 ± 29.6	0.35 ± 0.03	71.2 ± 3.2
	3	570.3 ± 45.9	0.34 ± 0.06	72.8 ± 3.7

$$^a\text{Entrapment efficiency (\%)} = \frac{\text{actual drug amount in liposomal dispersion after filtration}}{\text{theoretical drug amount in liposomal dispersion}} \times 100$$

Data are presented as mean ± standard deviation (SD) ($n = 3$).

Optimization of the temperature of solvent evaporation was conducted using simvastatin (SV) as model drug in the preliminary study. Preparation of SV-loaded proliposomes (SVPLs) was conducted at high (60°C) and low (40°C) temperature

of solvent evaporation (Table S1). The particle size and EE of reconstituted SV-loaded liposomes were evaluated (Table S2).

To determine SV concentration, reverse-phase HPLC was performed on a Waters e1515 system consisting of a 2487 dual λ absorbance detector (Waters Corporation, USA). For the chromatographic separation of SV, a Phenomenex Gemini-NX analytical column (250×4.6 mm, $5 \mu\text{m}$) was used. The wavelength for detection was set at 238 nm. The determination was carried out by isocratic elution using ACN / 20 mM phosphate buffer (pH 5.6) (80:20, v/v) mixture as the mobile phase at a flow rate of 1.0 mL/min. All samples were appropriately diluted with mobile phase prior to analysis.

The particle size and EE were variable among batches when the solvent evaporation conducted at high temperature (60°C). Meanwhile, the particle size and EE were even among batches when evaporation processed at low temperature (40°C). This might be resulted from the volume of solution before lyophilization. At 60°C , due to not only ethanol but also DDW was evaporated in rotary evaporator, the final volume of solution was different among batches, caused variability. However, at 40°C , DDW could not evaporated in rotary evaporator, the final volume before lyophilization was relatively consistent among batches, result in uniformity. Therefore, the evaporation condition was set to 40°C .

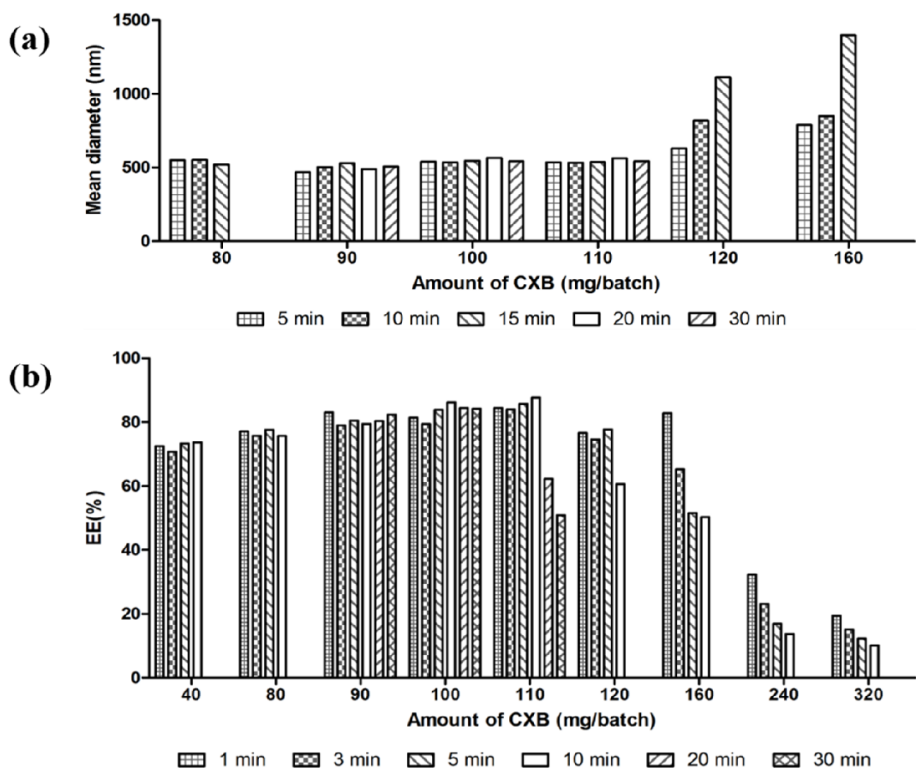


Figure S2. The effect of the amount of CXB in CXBPLs on the (a) mean diameter and (b) EE values after reconstitution.

The amount of CXB in CXBPLs was determined based on the mean diameter and EE of reconstituted CXB-loaded liposomes. As shown in Figure S2a, only the CXBPL batches with not more than 110 mg of CXB maintained their mean diameter for 30 min after reconstitution. Similarly, the CXBPL batches with not more than 100 mg of CXB maintained CXB-loaded liposomes (Figure S2b). The CXBPL batches with more than 110 mg of CXB showed CXB precipitation with time. Therefore, the amount of CXB in a batch of CXBPLs was set at 100 mg (Table 1).

Table S3

Solubility of VST in various media.

pH of buffer	pH 1.2	pH 4.0	pH 6.8	DDW
Solubility ($\mu\text{g/mL}$)	58.73 ± 0.98	272.19 ± 2.30	3108.96 ± 14.32	143.17 ± 1.07

Data are presented as mean \pm standard deviation (SD) ($n = 3$).

The solubility of VST at various pH was used to determine sink condition of *in vitro* dissolution studies (Table S2). Approximately 10 to 50 mg of VST was dispersed in 15mL of media at various pH (pH 1.2, 4.0, 6.8, and DDW) and vortexed for 30 min. Then, the tubes were incubated in a shaking water bath operated at 50 rpm at 37 °C. After 48 h incubation, the tubes were centrifuged at 3,000 rpm for 15 min (MF80, Hanil Science, Korea). An aliquot (1.4 mL) of supernatant was transferred to eppendorf tube and centrifuged at 13,200 rpm for 15 min (5415R, Eppendorf centrifuge, Germany). An aliquot (1 mL) of supernatant was filtered through a 0.2 μm syringe filter (Minisart RC15, Sartorius, Germany), and properly diluted prior to measuring the drug concentration by means of HPLC in the section 2.3.2.3. The volume of dissolution media for the study was chosen at 500 mL, except for pH 1.2 buffer at 1,000 mL to satisfy the sink condition according to 'USP 38 General

Information <1092> The Dissolution Procedure'.

Table S4

Solubility of CXB in various media.

% of SDS (w/v)	CXB solubility ($\mu\text{g/mL}$)				
	pH 1.2	pH 4.0	pH 6.8	pH 12.0	DDW
0.0	1.41 \pm 0.03	1.55 \pm 0.07	1.23 \pm 0.05	312.46 \pm 25.18	2.06 \pm 0.10
0.1	26.04 \pm 2.13	4.38 \pm 0.52	9.41 \pm 0.59	485.11 \pm 31.55	2.52 \pm 0.20
0.4	168.91 \pm 3.12	198.17 \pm 2.02	161.92 \pm 7.88	1168.53 \pm 33.21	129.86 \pm 4.74
0.7	289.23 \pm 5.52	385.12 \pm 5.45	331.54 \pm 10.59	1670.34 \pm 17.65	344.05 \pm 2.40
1.0	420.42 \pm 5.86	580.40 \pm 3.81	512.46 \pm 7.95	2271.35 \pm 41.36	545.56 \pm 14.21

Data are presented as mean \pm standard deviation (SD) ($n = 3$).

The solubility of CXB at various pH with various SDS concentration was evaluated to determine sink condition of *in vitro* dissolution studies (Table S3). The aqueous solubility of CXB was determined in various pH (pH 1.2, 4.0, 6.8, 12.0, and DDW) with 0.1%, 0.4%, 0.7%, and 1.0% (w/v) SDS. Approximately 3 mg of CXB was dispersed in 1.5 mL media and vortex-mixed for 30 min. Then, the tubes were incubated in a shaking water bath operated at 50 rpm at 37°C. After 48 h incubation, the tubes

were centrifuged at 13,200 rpm for 15 min, an aliquot (1 mL) of supernatant was filtered through a 0.2 µm syringe filter (Minisart RC15, Sartorius, Germany), and properly diluted prior to HPLC analysis as described at 2.3.2.3 section. The 500 mL of media with 0.4% (w/v) SDS was chosen for the dissolution tests.

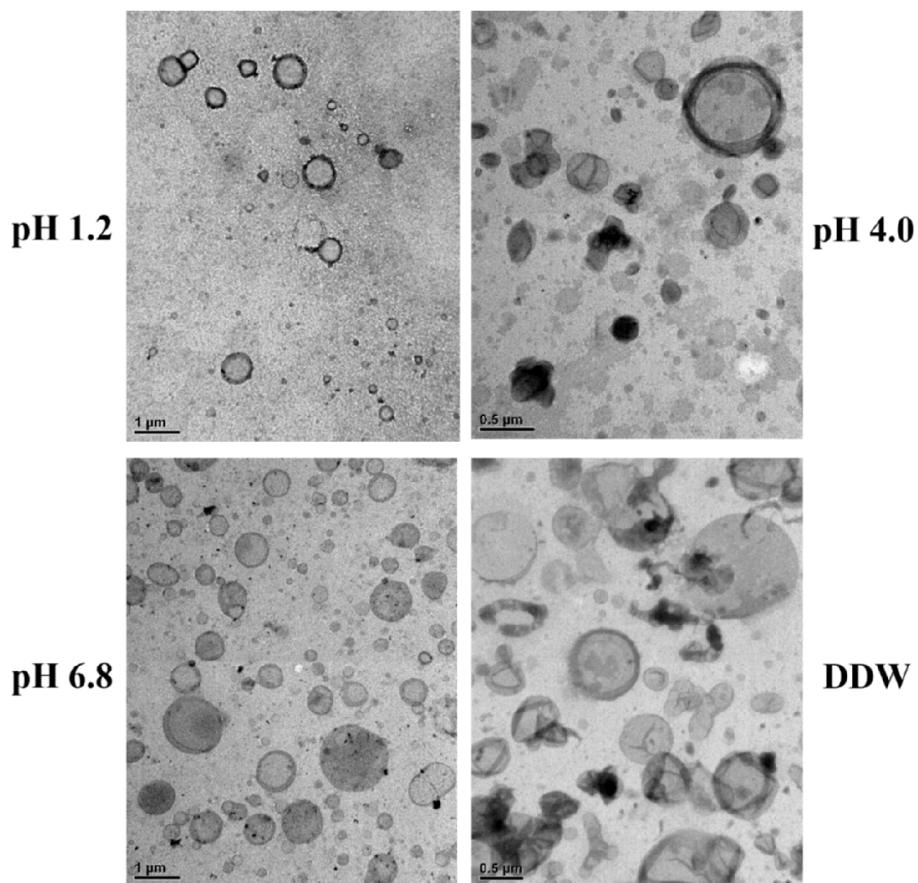


Figure S3. TEM images of VST-loaded liposomes in various dissolution media (pH 1.2, 4.0, 6.8, and DDW). The length of the scale bars are shown in Figure.

The reconstitution of VST-loaded liposomes from VSTPLs in various dissolution media (pH 1.2, 4.0, 6.8, and DDW) were observed by TEM as described in 2.3.2.1. Spherical liposomes were form in all dissolution media. The formation of liposomes could attribute to improve dissolution of VST of VSTPLs (Figure 5).

국문초록

향상된 경구 생체이용률을 위한 BCS

class II 약물의 프로리포솜 적용:

발사르탄과 세레콕시브

Purpose. 본 연구의 목적은 기존 제법보다 간편하면서도 높은 지질 함량을 갖는 프로리포솜 (Proliposomes, PLs) 제법을 개발하고, BCS class II 모델 약물로 발사르탄 (Valsartan, VST) 과 세레콕시브 (Celecoxib, CXB) 를 첨가한 프로리포솜을 제조 및 평가하는 것이다.

Methods. 회전 증발 응축기와 동결건조기를 사용하여 발사르탄이 봉입된 프로리포솜 (VSTPLs) 과 세레콕시브가 봉입된 프로리포솜 (CXBPLs) 을 제조하였다. 프로리포솜 제조에는 인체에 무독성한 원료 및 용매를 사용하여, 경구투여가 가능하게 하였다. 프로리포솜 내 최고 지질 비율을 확인하고 이를 바탕으로 VSTPLs와 CXBPLs의 조성을 설정하였다. 만들어진 프로리포솜은 주사 전자 현미경 (Scanning electron microscopy, SEM), X-선 회절계 (Powder X-ray diffractometer, PXRD), 시차 주사 열량측정계 (Differential scanning calorimetry, DSC)을 이용하여

고체 상태에서 평가하였다. 프로리포솜을 물에 풀어 재건한 리포솜 (liposomes) 의 입자도, 제타전위, 약물 봉입률 등을 평가하였고, 입자 성상은 투과전자현미경 (Transmission electron microscopy, TEM) 으로 확인하였다. 생체 외 (*in vitro*) 용출 및 랫에서의 생체 내 (*in vivo*) 약물동력학적 평가를 진행하였다.

Results. 상기 제법으로 프로리포솜 내의 지질 비율을 20% (w/w) 까지 증가시킬 수 있었다. 프로리포솜 내 약물은 결정형에서 무정형으로 변형되었다. 재건한 리포솜의 평균 입자경, 제타전위와 약물 봉입률은 VSTPLs에서 각각 369 ± 31 nm, -57.4 ± 0.4 mV, $77.5 \pm 2.8\%$ 이었으며, CXBPLs에서는 각각 537 ± 10 nm, -64.2 ± 0.3 mV, $84.7 \pm 1.2\%$ 이었다. 다양한 pH 환경에서 실시한 약물의 생체 외 (*in vitro*) 용출 평가에서는 프로리포솜 내의 약물이 원료 약물보다 더 빠르고 높은 용출을 보였다. 약물의 생체 내 (*in vivo*) 약물동력학 평가에서 프로리포솜이 원료 약물보다 더 높은 C_{max} 와 AUC 를 보였다.

Conclusions. 상기 제법으로 제조된 프로리포솜은 다음과 같은 장점을 지닌다. (a) 기존 제법보다 쉽고 공정 제어가 간단하며, (b) 사용된 원료와 용매가 무독성이며, (c) 만들어진 프로리포솜은 지질 비율이 높아 많은 양의 수불용성 약물을 봉입할 수 있으며, (d) 프로리포솜 내의 무정형으로 존재하는 약물과, 수상에서 빠르게 형성된 리포솜이 용출을 증가시키고 약물의 경구 생체이용률을 증가시키는 데에 기여한다.

주요어: Proliposomes, Valsartan, Celecoxib, Dissolution rate,
Oral bioavailability

학번: 2014-21972



저작자표시-비영리-변경금지 2.0 대한민국

이용자는 아래의 조건을 따르는 경우에 한하여 자유롭게

- 이 저작물을 복제, 배포, 전송, 전시, 공연 및 방송할 수 있습니다.

다음과 같은 조건을 따라야 합니다:



저작자표시. 귀하는 원저작자를 표시하여야 합니다.



비영리. 귀하는 이 저작물을 영리 목적으로 이용할 수 없습니다.



변경금지. 귀하는 이 저작물을 개작, 변형 또는 가공할 수 없습니다.

- 귀하는, 이 저작물의 재이용이나 배포의 경우, 이 저작물에 적용된 이용허락조건을 명확하게 나타내어야 합니다.
- 저작권자로부터 별도의 허가를 받으면 이러한 조건들은 적용되지 않습니다.

저작권법에 따른 이용자의 권리는 위의 내용에 의하여 영향을 받지 않습니다.

이것은 [이용허락규약\(Legal Code\)](#)을 이해하기 쉽게 요약한 것입니다.

[Disclaimer](#)

약학석사 학위논문

**Proliposomes for enhanced oral
bioavailability of BCS class II drugs:
valsartan and celecoxib**

향상된 경구 생체이용률을 위한 BCS class II

약물의 프로리포솜 적용: 발사르탄과

세레콕시브

2016 년 2 월

서울대학교 대학원

약학과 약제과학 전공

전 다 은

Abstract

Proliposomes for enhanced oral bioavailability of BCS class II drugs: valsartan and celecoxib

Daeun Jeon

Department of Pharmaceutics, College of Pharmacy

The Graduate School

Seoul National University

Purpose. The aim of this study was to develop a simple preparation method of proliposomes (PLs) with a high lipid content, and to characterize and evaluate the BCS class II drug-loaded PLs (valsartan-loaded PLs (VSTPLs) and celecoxib-loaded PLs (CXBPLs)) *in vitro* and *in vivo* for their suitability for oral delivery.

Methods. Rotary evaporator and freeze dryer were used to prepare PLs. Maximum lipid contents of PLs which can form liposomes after reconstitution were determined. After loading drugs, the solid state of PLs was also characterized by scanning electron microscopy (SEM), powder X-ray diffractometer (PXRD) and differential scanning calorimetry (DSC). PLs

were reconstituted with distilled water, and then were characterized by measuring the particle size, zeta potential, entrapment efficiency (EE), and drug content. Particle morphology of reconstituted liposomes was determined by transmission electron microscopy (TEM). *In vitro* dissolution and *in vivo* pharmacokinetics of PLs in rats were also evaluated.

Results. Phospholipid content of the PLs was increased up to 20% (w/w), thereby being able to enhance the drug loading content. Crystalline state of the drug was transformed to amorphous state during the preparation of PLs. Particle size of reconstituted VST-loaded liposomes and CXB-loaded liposomes were 369 ± 31 nm and 537 ± 10 nm with the zeta potential of -57.4 ± 0.4 mV and -64.2 ± 0.3 mV, respectively. The EE values of VST and CXB were $77.5 \pm 2.8\%$ and $84.7 \pm 1.2\%$ for VST-loaded liposomes and CXB-loaded liposomes, respectively. The rate and extent of dissolution of drugs from the PLs were higher than those of crude drug powder in various pHs. In pharmacokinetic studies after oral administration in rats, drugs in PLs showed higher C_{\max} values and 1.82-fold and 1.73-fold higher AUC values for VSTPLs and CXBPLs, respectively, than those from the drug powder. Shorter T_{\max} was shown in CXBPLs than that of crude drug powder.

Conclusions. The preparation method of PLs developed in this study has the following advantages compared with conventional preparation methods: (a) the preparation method is simple and could be easily scaled up, (b) the solvent system used has no toxicity concern, (c) the PLs have a higher lipid content, which can enhance the incorporation of poorly water-soluble drugs, (d) the rapid formation of liposomes in aqueous media and the amorphous state of the drug in PLs can increase solubility and dissolution rate, thereby increase oral

bioavailability of the drug.

Keywords: Proliposomes, Valsartan, Celecoxib, Dissolution rate, Oral
bioavailability

Student Number: 2014-21972

Table of Contents

Abstract	i
List of Tables	vi
List of Figures	vii
List of Tables and Figures of Supplementary Information	viii
1. Introduction	1
2. Materials and methods	4
2.1 Materials.....	4
2.2 Preparation of proliposomes (PLs).....	4
2.3 Characterization of PLs.....	5
2.3.1 Solid state characterization	5
2.3.1.1 Field emission scanning electron microscopy (FESEM).....	5
2.3.1.2 Differential scanning calorimetry (DSC).....	5
2.3.1.3 Powder X-ray diffractometry (PXRD).....	6
2.3.2 Characterization of liposomes.....	6
2.3.2.1 Transmission electron microscopy (TEM).....	6
2.3.2.2 Particle size and zeta potential.....	6
2.3.2.3 Determination of drug content and entrapment efficiency (EE).....	7
2.4 <i>In vitro</i> dissolution studies	8
2.4.1 <i>In vitro</i> dissolution studies of VSTPLs	8
2.4.2 <i>In vitro</i> dissolution studies of CXBPLs	9
2.5 <i>In vivo</i> pharmacokinetic studies	10
2.5.1 <i>In vivo</i> pharmacokinetic studies of VSTPLs.....	10

2.5.2 <i>In vivo</i> pharmacokinetic studies of CXBPLs	11
2.5.3 Pharmacokinetic parameters	13
2.6 Statistical Analysis	13
3. Result and discussion	14
3.1. Preparation of proliposomes (PLs).....	14
3.2 Characterization of PLs	15
3.2.1 Solid state characterization	15
3.2.2 Characterization of liposomes.....	17
3.3 <i>In vitro</i> dissolution studies	17
3.3.1 <i>In vitro</i> dissolution studies of VSTPLs	17
3.3.2 <i>In vitro</i> dissolution studies of CXBPLs	18
3.4 <i>In vivo</i> pharmacokinetic studies	19
3.4.1 <i>In vivo</i> pharmacokinetic studies of VSTPLs.....	19
3.4.2 <i>In vivo</i> pharmacokinetic studies of CXBPLs	20
4. Conclusions	22
5. References.....	23
Supplementary Information	40
국문초록	49

List of Tables

Table 1. Composition of the developed proliposomal formulations.....	28
Table 2. Characterization of the developed proliposomal formulations	29
Table 3. Pharmacokinetic parameters of valsartan (VST) after oral administration of crude VST powder and VSTPLs at a dose of 3 mg/kg in rats	30
Table 4. Pharmacokinetic parameters of celecoxib (CXB) after oral administration of crude CXB powder, Celebrex, and CXBPLs at a dose of 2 mg/kg in rats.....	31

List of Figures

Figure 1. Schematic illustration of the preparation method of PLs.....	32
Figure 2. SEM images of sorbitol, VST, CXB, Celebrex, VSTPLs, and CXBPLs. The lengths of the scale bars are 1 μm	33
Figure 3. Characterization of VSTPLs and CXBPLs. (a) DSC thermograms and (b) X-ray diffraction patterns.....	34
Figure 4. Size distribution and TEM images of the liposomes after reconstitution of blank PLs, VSTPLs, and CXBPLs. The length of the scale bars are 0.5 μm	35
Figure 5. <i>In vitro</i> dissolution profiles of crude VST powder and VSTPLs at pH 1.2, 4.0, 6.8, and DDW. Data are presented as the mean \pm SD ($n = 3$)...	36
Figure 6. <i>In vitro</i> dissolution profiles of crude CXB powder, Celebrex, and CXBPLs at pH 1.2, 4.0, 6.8, and 12.0. Data are presented as the mean \pm SD ($n = 3$).....	37
Figure 7. Plasma concentration vs. time profiles of VST after a single oral administration of crude VST powder and VSTPLs at a dose of 3 mg/kg. The values are presented on a (a) semilogarithmic plot and (b) linear scale. Data are presented as the mean \pm SD ($n \geq 3$).....	38
Figure 8. Plasma concentration vs. time profiles of CXB after a single oral administration of crude CXB powder, Celebrex, and CXBPLs at a dose of 2 mg/kg. The values are presented on a (a) semilogarithmic plot and (b) linear scale (inset: expanded view form time 0 to 250 min). Data are presented as the mean \pm SD ($n \geq 3$).....	39

List of Tables and Figures of Supplementary Information

Figure S1. Images of PLs prepared (a) without solvent evaporation step and (b) with the 25% (w/w) of lipid content.....	40
Table S1. Composition and evaporation temperature of simvastatin-loaded proliposomes (SVPLs).....	41
Table S2. Characterization of SVPLs.....	42
Figure S2. The effect of the amount of CXB in CXBPLs on the (a) mean diameter and (b) EE values after reconstitution.....	44
Table S3. Solubility of VST in various media.....	45
Table S4. Solubility of CXB in various media.....	46
Figure S3. TEM images of VST-loaded liposomes in various dissolution media (pH 1.2, 4.0, 6.8, and DDW). The length of the scale bar is shown in Figure	48

1. Introduction

More than 40% of new chemical entities (NCE) have poor aqueous solubility [1]. Since aqueous solubility is essential for drugs to enter the systemic circulation and show medicinal effect, the poor solubility of drugs is an issue to solve in drug development [2]. Drugs with poor water solubility (biopharmaceutical system (BCS) class II and IV) could suffer from low bioavailability [1, 3]. Therefore, several attempts have been made to increase solubility of drug to improve oral bioavailability such as solid dispersion [4-6], emulsion [2], spherical agglomeration [7], nanosuspension [8], nanoparticles [9], spray-drying [10], and liposomes [11].

Among these formulation strategies to increase the solubility of drugs, lipid-based drug delivery systems, such as liposomes, have been widely used for increasing solubility, improving dissolution, and enhancing oral bioavailability of drugs [2]. Liposomes are vesicular system composed of phospholipid, which could encapsulate lipophilic to hydrophilic compounds, small- to macro-molecules [12]. The absorption mechanisms of drug associated with liposomes in the gastrointestinal tract are: (a) liposomes could be absorbed by endocytosis, (b) liposome-vesicles could adsorb to mucosal membrane and fuse with the cell membrane, (c) drugs released from liposomes could enter cell *via* micropinocytosis, (d) liposomes could alter the colloidal environment of intestinal milieu by forming mixed micelles and micelles with physiological bile salts [13-15]. However, liposomes have stability problems such as susceptibility to hydrolysis and oxidation of lipid layer, vesicle

aggregation, fusion and sedimentation related to leakage of entrapped drugs [3, 12, 13].

To overcome the instability of liposomes, the concept of proliposomes (PLs) was adopted. PLs are dry, free flowing powder which could form more uniform-sized liposomes over conventional liposomes by hydration [3, 12]. Since PLs are dry formulation, they could prevent vesicle aggregation and fusion during storage [16]. Being available in dry powder form, further modification is easy (e.g. tableting or capsule filling after mixing with other pharmaceutical excipients) [12, 17]. Also, PLs showed enhanced dissolution and improved bioavailability of drugs [3, 18]. Various preparation methods of PLs were established using rotary evaporator [16, 19], spray dryer [13], fluidized bed [20], and supercritical anti-solvent technology [21]. These conventional methods are in need of specific equipment (e.g. spray dryer, fluidized bed granulator) and the procedures are complicated to control [12].

The aim of this present study were to (a) develop a simple method to prepare PLs (b) evaluate the resultant PLs incorporating BCS class II model drug: valsartan (VST) and celecoxib (CXB). VST is an orally active highly selective angiotensin II type 1 receptor antagonist used for the treatment of hypertension [22]. VST has relatively low bioavailability (~25%) caused by its poor aqueous solubility [2, 22]. CXB is a selective cyclooxygenase 2 (COX-2) inhibitor for treatment of arthritis and acute pain [4]. CXB has incomplete and highly variable oral bioavailability caused by its low water solubility (~ 5 µg/mL) [4]. VST and CXB are categorized as BCS class II drugs which have high permeability but low solubility [3, 4]. Applying proliposomal formulations to BCS class II drugs, the solubility and dissolution of drugs

could be increased, thereby enhancing oral bioavailability of drugs.

2. Materials and methods

2.1. Materials

VST was purchased from Tecoland (Irvine, CA). CXB and Celebrex were kindly gifted by Hanlim Pharm. Co., Ltd. (Seoul, Korea). Soy phosphatidyl choline (SPC) was a gift from PHYTOS (Gyeonggi, Korea). Anhydrous ethanol of 99.9% purity was purchased from Daejung (Gyeonggi, Korea). Poloxamer 188 was purchased from BASF (Ludwigshafen, Germany), sorbitol sodium dodecyl sulfate (SDS) was purchased from Sigma–Aldrich (St. Louis, MO). All other reagents were of analytical grade.

2.2. Preparation of proliposomes (PLs)

VST-loaded proliposomes (VSTPLs) and CXB-loaded proliposomes (CXBPL) were prepared by rotary evaporator and freeze-dryer (Figure 1). Briefly, SPC (800 mg), poloxamer 188 (40 mg), and VST (160 mg) or CXB (100 mg) were dissolved in ethanol (8.75 ml). The mixture was vortex-mixed and sonicated to obtain a clear yellow solution. Sorbitol (3160 mg) was dissolved in double-deionized water (DDW) (3.75 ml). The two solutions were mixed in a round-bottom flask with gentle stirring for 30 min. The mixture was then evaporated under vacuum for 10 min at 40°C using a rotary evaporator. After removing ethanol, the resulting solution was immediately lyophilized over 24 h. The obtained PLs were ground using a pestle and mortar.

The powder which passed through the sieve of 25 mesh size but could not pass through 100 mesh size was collected. The pale-yellow powder was stored at -4°C for further experiments. The blank PLs were prepared following the same methods without drugs.

2.3 Characterization of PLs

2.3.1 Solid state characterization

2.3.1.1 Field emission scanning electron microscopy (FESEM)

The particle morphology of sorbitol, Celebrex, VST, CXB, VSTPLs, and CXBPLs were characterized by FESEM. The micrographs were recorded on a JSM-6700F from JEOL (Japan). For FESEM measurement, the samples were placed on carbon tape and sputter-coated with a thin layer of platinum for 120 sec prior to measurements. The coated samples were randomly scanned and photomicrographs were taken with FESEM.

2.3.1.2 Differential scanning calorimetry (DSC)

DSC experiments were conducted using DSC-Q1000 (TA Instrument, UK). Accurately weighed samples were scanned from 0°C to 200°C with a scan speed of 10°C/min.

2.3.1.3 Powder X-ray diffractometry (PXRD)

PXRD was used to assess the degree of crystallinity of drugs and other raw materials before and after preparing PLs. The analysis was carried out using a D8 ADVANCE with DAVINCI (BRUKER, German) Cu α_1 radiation (1.5418 Å). An acceleration voltage and current of 40 kV and 40 mA were used, respectively. Samples were scanned between 3 ° and 50 ° with a step size of 0.02 ° and a scan speed of 0.5 sec/step.

2.3.2 Characterization of liposomes

2.3.2.1 Transmission electron microscopy (TEM)

Reconstituted liposomal dispersion was made by putting 10 mg of PLs into 1 mL of DDW and agitating with hand for 5 min. For TEM measurement, a drop of dispersion was placed onto a surface of a 200 mesh carbon-coated copper grid (Electron Microscopy Sciences, USA). The liposome particles settled on the grid were negatively stained with uranyl acetate. The excess DDW was removed with a filter paper and left to dry at room temperature. Then, the grid was loaded into TEM (JEM1010, Jeol, Japan) and investigated at 80 kV.

2.3.2.2 Particle size and zeta potential

The particle size and zeta potential of reconstituted liposomes were evaluated by electrophoretic light scattering spectrophotometer (ELS-Z,

Otsuka Electronics, Japan).

2.3.2.3 Determination of drug content and entrapment efficiency (EE)

To determine drug content of PLs, 10 mg of drug-loaded PLs were dissolved in 50% acetonitrile (ACN) with bath sonication. The drug concentration of the sample was determined by the HPLC method described below. The drug content was calculated from the following equation:

$$\text{Drug content (\%)} = \frac{\text{actual drug amount in proliosomes}}{\text{total weight of proliosomes}} \times 100$$

To determine EE after reconstitution with DDW, 10 mg/mL of drug-loaded PLs were made with gentle handshaking for 5 min and filtered through 0.45 μm syringe filter (Minisart RC15, Sartorius, Germany) to remove undissolved drug. An aliquot (100 μL) of filtered dispersion was diluted with 900 μL of ACN to break down liposomes and dissolve drugs which were entrapped into the liposomes. The concentration of drug of the samples was determined by following HPLC method. The drug entrapment efficiency (EE) was calculated from the following equation:

$$\text{EE (\%)} = \frac{\text{actual drug amount in liposomal dispersion after filtration}}{\text{theoretical drug amount in liposomal dispersion}} \times 100$$

To determine the VST concentration, reverse-phase HPLC was performed on a Waters e2695 system consisting of a 2475 multi λ fluorescence detector (Waters Corporation, USA). For the chromatographic separation of VST, a Phenomenex Gemini-NX analytical column (250 \times 4.6 mm, 5 μ m) was used with isocratic elution using ACN with 0.025% trifluoroacetic acid (TFA) / 5 mM phosphate buffer (pH 2.5) with 0.025% TFA (70:30, v/v) mixture as the mobile phase at a flow rate of 1.0 mL/min. The wavelength for detection was set at 234 nm and 378 nm for excitation and emission, respectively. All samples were appropriately diluted with the mobile phase prior to analysis.

To determine the CXB concentration, reverse-phase HPLC was performed on a Waters e1525 system consisting of a 2487 dual λ absorbance detector (Waters Corporation, USA). For the chromatographic separation of CXB, a Phenomenex Gemini-NX analytical column (250 \times 4.6 mm, 5 μ m) was used with isocratic elution using ACN with 0.1% triethylamine (TEA) / pH 9.0 10 mM phosphate buffer with 0.1 % TEA (70:30, v/v) mixture as the mobile phase at a flow rate of 1.0 mL/min. The wavelength for detection was set at 260 nm. All samples were appropriately diluted with the mobile phase prior to analysis.

2.4 *In vitro* dissolution studies

2.4.1 *In vitro* dissolution studies of VSTPLs

The dissolution of VSTPLs and crude VST powder were tested using a USP

type II (paddle) dissolution apparatus (Electrolab TDT-08L, India). DDW, pH 1.2, 4.0, and 6.8 buffer media were used as a different dissolution media at a temperature of $37.0 \pm 0.2^\circ\text{C}$ and a paddle speed of 50 rpm. Crude VST powder or VSTPLs (equivalent to 10 mg of VST) was encapsulated into hard capsules and the filled capsules were added to dissolution medium with sinker. The volume of dissolution medium was 500 mL for DDW, pH 4.0, and pH 6.8 buffer, and 1000 mL for pH 1.2 buffer to maintain the sink condition (Table S3). Aliquots of samples (5 mL) were withdrawn from the dissolution vessel at predetermined time intervals (5, 10, 20, 30, 45, 60, 90, and 120 min) and the same volume of fresh medium was added to maintain constant volume of dissolution medium. The withdrawn samples were passed through a $0.45\ \mu\text{m}$ syringe filter to remove undissolved VST. An aliquot of filtrate was properly diluted and analyzed by HPLC as described in 2.3.2.3 section.

2.4.2 *In vitro* dissolution studies of CXBPLs

The dissolution of CXBPLs, Celebrex, and crude CXB powder were tested using a USP type II (paddle) dissolution apparatus (Electrolab TDT-08L, India) at various pH (pH 1.2, 4.0, 6.8 and 12.0). Buffer media (500 mL) containing 0.4% (w/v) SDS were used (Table S4) at a temperature of $37 \pm 0.2^\circ\text{C}$ with paddle rotating at a speed of 50 rpm. Each formulation equivalent to 2 mg of CXB was encapsulated into hard capsules. The filled capsules were added to dissolution medium with sinker. Samples (1 mL) were withdrawn from the dissolution vessel at predetermined time intervals (15, 30, 45, 60, 90, and 120 min) and equal volume of fresh medium was replaced. Samples were filtered

through a 0.45 μ m syringe filter to remove undissolved CXB. The filtrate was properly diluted and analyzed by HPLC as described in 2.3.2.3 section.

2.5 *In vivo* pharmacokinetic studies

2.5.1 *In vivo* pharmacokinetic studies of VSTPLs

A pharmacokinetic study in Sprague-Dawley rats was designed to evaluate the VSTPL by comparison with the crude VST powder at a 3 mg/kg dose. The rats, weighing 235 \pm 5 g, were housed in compliance with good laboratory practice (GLP). The rats were fasted for at least 12 h prior to dosing but had free access to water. The rats were randomly divided into 2 treatment groups ($n \geq 3$). Each formulation was encapsulated into #9 hard gelatin capsule (Torpac, USA). Each capsule and following 1 mL of DDW was administered orally. After administration, 250 μ L of blood sample were obtained at predetermined time intervals (10, 20, 30, 45, 60, 90, 120, 240, and 480 min). The samples were immediately centrifuged at 4°C and 13,200 rpm for 2.5 min (5415R, Eppendorf centrifuge, Germany), and an aliquot (100 μ L) of supernatant plasma sample was collected and were stored below -20°C until further analysis.

To determine the VST concentration in rat plasma, pretreatment was conducted before analysis. The frozen samples were thawed at 37°C, and 100 μ L of plasma sample was mixed with 1 mL of internal standard solution (losartan, 5 μ g/mL in ACN) and vortex-mixed for 30 min. The sample was

then centrifuged at 13,200 rpm for 5 min. An aliquot (900 μ L) of the supernatant was separated and fluid was evaporated at 60°C under nitrogen gas purge. The residue was reconstituted with 50 μ L of 50% ACN, vortex-mixed for 10 min, centrifuged at 9,000 rpm for 30 sec, and 45 μ L of supernatant was collected for HPLC analysis.

A 10 μ L aliquot of prepared sample was injected into a Phenomenex Gemini-NX analytical column (250 \times 4.6 mm, 5 μ m) and eluted isocratically, using an 0.025% TFA in ACN / 0.025% TFA in 5mM phosphate buffer (pH 2.5) (60:40, v/v) mixture as a mobile phase, at a flow rate of 1.0 mL/min. The HPLC system used was Waters e2695 system consisting of a 2475 multi λ fluorescence detector (Waters Corporation, USA). The wavelength for VST detection was set at 234 nm and 378 nm for excitation and emission wavelengths, respectively.

2.5.2 *In vivo* pharmacokinetic studies of CXBPLs

A pharmacokinetic study in Sprague-Dawley rats was designed to evaluate the CXBPLs by comparison with Celebrex and the crude CXB powder at a 2 mg/kg dose. The rats, weighing 248 \pm 23 g, were housed in compliance with good laboratory practice (GLP). The rats were fasted for at least 12 h prior to dosing but had free access to water and were randomly divided into 3 treatment groups ($n \geq 3$). Each formulation equivalent to 2mg/kg of CXB was encapsulated into #9 hard gelatin capsule. Each capsule was administered orally at a single dose via an oral gavage. At predetermined time intervals (1, 5, 15, 30, 45, 60, 90, 120, 240, 360, 480 and 1440 min), 120 μ L of blood

sample were obtained and immediately centrifuged at 4°C and 13,200 rpm for 2.5 min (5415R, Eppendorf centrifuge, Germany) and an aliquot (50 µL) of supernatant plasma sample was collected and were stored below -20°C until further analysis.

Before analysis, the frozen samples were thawed at 37°C and spiked with 200 µL internal standard solution (VST, 100 ng/mL in ACN) and vortex-mixed for 5 min. The mixtures were centrifuged at 4°C and 13,200 rpm for 5 min, and 160 µL of supernatant was collected for LC/MS/MS analysis.

HPLC analysis was carried out using an Agilent Technologies 1260 Infinity HPLC system (Agilent Technologies, Inc.; Palo Alto, CA, USA), equipped with a G1312B binary pump, a G1367E autosampler, a G1316C thermostatted column compartment, and a G1330B thermostat. Chromatographic separation was achieved using a Agilent Poroshell 120 EC-C18 column (50 × 4.6 mm, 2.7 µm; Agilent Technologies) with a C18 guard column (4 mm × 2.0 mm; Phenomenex; CA, USA) with 5 µL of sample injection volume. The isocratic mobile phase is consisted of ACN and 5 mM ammonium formate buffer (95:5, v/v), at a flow rate of 0.4 mL/min. Mass analysis was performed at negative electrospray ionization (ESI) mode on an Agilent Technologies 6430 Triple Quad LC/MS system. The mass transitions from precursor to product ion, collision energy, and fragmentor voltage were m/z 380.2 → 316.2, 19 eV, and 170 V for CXB and m/z 434.1 → 350.0, 18 eV, and 140 V for VST, respectively. The retention times of CXB and VST were 1.8 and 1.5 min, respectively. MassHunter Workstation Software Quantitative Analysis (Version B.05.00; Agilent Technologies, Inc.) were used for data acquisition and processing.

2.5.3 Pharmacokinetic parameters

Plasma concentration of drug in rats were plotted against time, and the pharmacokinetic parameters were calculated using a non-compartmental model *via* WinNonlin software (version 3.1, Pharsight Corporation, USA). The area under the plasma concentration versus time curve from time zero to infinity (AUC) was obtained by the log-linear trapezoidal method, the peak plasma concentration of drug (C_{\max}), the time taken to reach the peak concentration (T_{\max}), and the elimination half-life ($t_{1/2}$) were obtained from the individual plasma concentration-time curve.

2.6 Statistical analysis

All experimental data were expressed as mean \pm standard deviation (S.D.). The statistical analysis was carried out using Student's *t*-test and one-way analysis of variance (ANOVA). The level of statistical significance was defined by $p < 0.05$. All experiments were conducted more than three times except for Figure S2.

3. Result and discussion

3.1. Preparation of PLs

VSTPLs, CBXPLs, and blank PLs were successfully prepared by using rotary evaporator and freeze dryer. Every raw material of PLs was dissolved into water-ethanol mixture. Ethanol was chosen as organic solvent because it is Class 3 residual solvent in '*USP 38 General Chapter <467> Residual Solvents*' which is regarded as less toxic and have low risk to human health.

This method has several strong points than conventional preparation method: (a) it has few process parameters than conventional preparation method including spray drying method, fluidized bed method, and super critical anti-solvent method, (b) the phospholipid content of the PLs could be increased.

Solvent evaporation process was introduced to remove only ethanol in the mixture and make aqueous solution. Heterogeneous proliposomal formulation was obtained when water-ethanol mixture went through lyophilization, because each solvent has its different sublimation temperature (Figure S1a). Low temperature (40°C) of solvent evaporation process attribute to consistent reproducibility of PLs (Table S2). Therefore, solvent evaporation is significant step to yield homogeneous proliposomal formulation. Lyophilization was adopted to remove remaining DDW in the formulation.

Sorbitol is widely used water soluble matrix in preparing proliposomal formulation [16, 23]. The high dissolution rate of porous sorbitol could result in rapid formation of spherical liposomes after reconstitution than other water

soluble matrices [23]. Poloxamer 188 was added to increase the stability of reconstituted liposomes [24]. To increase the amount of reconstituted drug-loaded liposomes in unit weight of the formulation, a high lipid to matrix ratio of PLs is desirable. By this method, the lipid content could be increased up to 20% (w/w). When the lipid content was increased up to 25% (w/w), the formulation had sticky property which was hard to modify further (e.g. grinding, capsule filling) (Figure S1b). Finally, the weight ratio of blank PLs was set at sorbitol/SPC/poloxamer 188 = 79/20/1. Drugs were added to the blank PLs formulation based on the preliminary study to set the amount of drugs added (Figure S2). The final composition of VSTPLs, CXBPLs, and blank PLs were shown in Table 1.

3.2 Characterization of PLs

3.2.1 Solid state characterization

The surface morphology of sorbitol, drugs, and PLs was evaluated by FESEM, as shown in Figure 2. Sorbitol showed porous structure [23]. VST had a rectangular crystalline structure [6], and CXB showed needle-shaped crystalline [25]. However, the characteristic structure of the drugs and sorbitol was disappeared after preparing into PLs.

The thermal behaviors of the drugs, excipients, and prepared PLs were shown in Figure 3a. A sharp endothermic peak was shown at around 103°C for VST, which was corresponded its melting temperature [1]. The DSC curve

for CXB showed an endothermic peak at around 160°C which is related to its melting temperature [26]. The characteristic endothermic peak of CXB was also shown in the DSC curve of Celebrex [10], indicating the crystalline state of CXB in Celebrex. Sorbitol and poloxamer 188 had their own endothermal peak which are similar to those reported in the previous reports [4, 27]. However, all those characteristic peaks were absent in thermograms of PLs, which illustrates that the crystalline drugs have changed into amorphous form during the preparation of PLs.

For further determination of the crystallinity of drugs in the formulation, the PXRD analysis was conducted and the diffractograms were shown in Figure 3b. As expected from DSC results, drugs and other excipients had their own characteristic peaks [4, 6, 26, 28], but the PLs showed a series of broad peaks. The characteristic peaks of drugs were absent in PXRD spectra of VSTPLs and CXBPLs in comparison with those of blank PLs. This indicates that the drugs entrapped in PLs were in an amorphous state, which agreed well with the DSC results.

Taken together, the drugs have changed from crystalline state to amorphous state during the preparation of PLs. The amorphous form of drugs could provide increased solubility and higher dissolution rate which might result in better bioavailability due to the higher free energy of the amorphous drug [1, 5, 29]. This was further illustrated by the *in vitro* dissolution tests and *in vivo* pharmacokinetic studies. The amorphous state of drugs in PLs maintained for at least 15 months and 5 months of low temperature (~ -20°C) storage period for VSTPLs and CXBPLs, respectively (Figure 3).

3.2.2 Characterization of liposomes

By adding DDW and manual agitation of PLs, about 370 nm and 540 nm of liposomes from VSTPLs and CXBPLs, respectively, were made (Table 2). The successful reconstitution to spherical liposomal suspension from PLs was confirmed by TEM observation (Figure 4). The prepared liposomes showed about -60 mV zeta potential values (Table 2). The negative zeta potential would suggest non-aggregated physical stability of reconstituted liposomal suspension [30, 31]. The EE of reconstituted liposomes was about 78% and 85% for VSTPLs and CXBPLs, respectively (Table 2).

3.3 *In vitro* dissolution studies

3.3.1 *In vitro* dissolution studies of VSTPLs

The dissolution profile of VST from VSTPLs and crude VST powder in various pH are depicted in Figure 5. The dissolution tests were carried out at various dissolution media (pH 1.2, 4.0, 6.8 and DDW). Each dissolution medium maintained the sink condition during the experiments (Table S3). The dissolved drug of crude VST powder were below 50% in all dissolution media, excluding at pH 6.8 because of the pH-dependent solubility of VST due to its weak acidity [1, 32]. However, VST dissolved from VSTPLs was increased compared to that of crude VST powder in all media. The increased dissolution of VST from VSTPLs might be due to the increased solubility of the

amorphous state of VST in the VSTPLs, as evidenced by the DSC and PXRD results, or VSTPLs formed VST-loaded liposomal dispersion by contacting dissolution medium, as consistent with the TEM results (Figure S3). Moreover, the improved dissolution at low pH might be helpful for enhanced absorption since the low bioavailability of VST is resulted by poor solubility of VST in acidic environment of the gastrointestinal tract [22].

3.3.2 *In vitro* dissolution studies of CXBPLs

The dissolution profiles of CXB from crude CXB powder, Celebrex, and CXBPLs in various pH are illustrated in Figure 6. The dissolution test were conducted at various dissolution media (pH 1.2, 4.0, 6.8 and 12.0). Each dissolution medium maintained the sink condition by adding 0.4% (w/v) SDS in all dissolution media (Table S4). The dissolved CXB from crude CXB powder was less than 30% in all dissolution media, except at pH 12.0 due to its weak acidity ($pK_a \approx 11.1$) [33]. The dissolution rate of Celebrex increased as the pH of dissolution medium increased. This might be due to the SDS in Celebrex formulation, which attribute the increased solubility of CXB, and croscarmellose sodium, which is used as a disintegrant. However, at pH 1.2, the dissolution rate of Celebrex was similar to that of crude CXB powder, which might be due to the lack of swelling property of croscarmellose sodium at low pH [34]. Remarkable dissolution enhancement was observed in CXBPLs at all dissolution medium. The dissolved CXB from CXBPLs showed more than 50% within 30 min and 100% in 120 min at all dissolution medium. The increased dissolution of CXB from CXBPLs might be due to (a)

the conversion to amorphous form from crystalline state of CXB in the CXBPLs during preparation (b) the CXB-loaded liposomes were formed quickly from CXBPLs by adding dissolution medium. Since CXB is a BCS class II drug which has poor drug absorption due to its poor dissolution property [8], the improved dissolution rate of CXBPLs would be helpful for enhanced oral bioavailability of CXB.

3.4 *In vivo* pharmacokinetic studies

3.4.1 *In vivo* pharmacokinetic studies of VSTPLs

The *in vivo* pharmacokinetics after oral administration of crude VST powder and VSTPLs were determined in rats. The plasma concentration versus time profiles were illustrated and pharmacokinetic parameters were listed in Figure 7 and Table 3. The VSTPL-treated group exhibited 1.88-fold and 1.82-fold higher C_{\max} and oral absorption (AUC), respectively, compared to those of crude VST powder-treated group ($p < 0.05$). The higher plasma concentration and systemic exposure of VST in VSTPL-treated group might be due to the increased dissolution rate in acidic pH, which are corresponded to *in vitro* dissolution results, together with other mechanisms proposed in the previous reports such as mixed-micelle formation with endogenous bile acids [14, 35]. The $t_{1/2}$ values of two groups were about the same (data not shown).

3.4.2 *In vivo* pharmacokinetic studies of CXBPLs

The *in vivo* pharmacokinetic study was carried on crude CXB powder, Celebrex, and CXBPLs in rats. Each formulation was administered orally and the plasma concentration of CXB was analyzed. The plasma CXB concentration versus time curve and pharmacokinetic parameters were shown in Figure 8 and Table 4. As expected in the *in vitro* dissolution tests, the systemic exposure (AUC) of CXBPL-treated group was significantly increased by 1.73-fold in comparison with the crude CXB powder-treated group ($p < 0.05$). The increased oral absorption might be due to various possible mechanisms such as mixed-micelle formation with endogenous bile acids in the gastrointestinal tract [14, 35], or might be due to increased dissolution rate by forming liposomal suspension in the gastrointestinal fluid and increased solubility of amorphous CXB of CXBPLs. The Celebrex-treated group exhibited significantly increased AUC (1.67-fold) compared to crude CXB-treated group ($p < 0.05$), as well. The increase of oral absorption of Celebrex might be attributed from the excipients such as SDS and disintegrants which might have been helpful for improving dissolution rate of CXB. However, the rank order of T_{max} from fastest to slowest and C_{max} from highest to lowest was as follows: CXBPLs > Celebrex > crude CXB powder. CXB can be absorbed throughout the gastrointestinal tract [36]. The T_{max} is related to *in vitro* dissolution rate of each formulation at physiologically relevant pH media (pH 1.2, 4.0, and 6.8). The rapid and high extent of dissolution of CXB in physiological pH might contribute to shorter T_{max} and higher C_{max} . There were no significant differences in $t_{1/2}$ values among three

groups (data not shown).

4. Conclusion

BCS class II drugs-loaded proliposomes with 20% (w/w) of lipid content were successfully prepared with simpler preparation method than convention methods. Solvent evaporation at low temperature (40°C) and lyophilization were used to remove solvent and yielded homogeneous formulation. The crystalline state of drugs has changed to amorphous form by preparing proliposomal formulation, which attributed to increased dissolution rate of drug-loaded PLs. The PLs rapidly formed liposomal suspension by adding water or dissolution medium, which also attributed to improved dissolution rate. Since the oral bioavailability of BCS class II drugs is limited to their poor dissolution, formulation which increase drug dissolution could improve oral absorption of BCS class II drugs. The enhanced oral bioavailability of drug-loaded PLs compared with crude drug powder was confirmed in rats. Taken together, the developed proliposomes offers a new approach to improve the oral absorption of BCS class II drugs like VST and CXB.

5. References

1. Ma, Q., et al., *Uniform nano-sized valsartan for dissolution and bioavailability enhancement: influence of particle size and crystalline state*. International Journal of Pharmaceutics, 2013. **441**(1-2): p. 75-81.
2. Baek, I.H., et al., *Oral absorption of a valsartan-loaded spray-dried emulsion based on hydroxypropylmethyl cellulose*. International Journal of Biological Macromolecules, 2014. **69**: p. 222-8.
3. Yanamandra, S., et al., *Proliposomes as a drug delivery system to decrease the hepatic first-pass metabolism: case study using a model drug*. European Journal of Pharmaceutical Sciences, 2014. **64**: p. 26-36.
4. Homayouni, A., et al., *Preparation and characterization of celecoxib solid dispersions; comparison of poloxamer-188 and PVP-K30 as carriers*. Iranian Journal of Basic Medical Sciences, 2014. **17**(5): p. 322-31.
5. Mosquera-Giraldo, L.I., Trasi, N.S., and Taylor, L.S., *Impact of surfactants on the crystal growth of amorphous celecoxib*. International Journal of Pharmaceutics, 2014. **461**(1-2): p. 251-7.
6. Yan, Y.D., et al., *Novel valsartan-loaded solid dispersion with enhanced bioavailability and no crystalline changes*. International Journal of Pharmaceutics, 2012. **422**(1-2): p. 202-10.
7. Gupta, V.R., et al., *Spherical crystals of celecoxib to improve solubility, dissolution rate and micromeritic properties*. Acta Pharmaceutica, 2007. **57**(2): p. 173-84.

8. Dolenc, A., et al., *Advantages of celecoxib nanosuspension formulation and transformation into tablets*. International Journal of Pharmaceutics, 2009. **376**(1–2): p. 204-12.
9. Liu, Y., et al., *Mechanism of dissolution enhancement and bioavailability of poorly water soluble celecoxib by preparing stable amorphous nanoparticles*. Journal of Pharmacy and Pharmaceutical Sciences, 2010. **13**(4): p. 589-606.
10. Lee, J., et al., *Enhanced dissolution rate of celecoxib using PVP and/or HPMC-based solid dispersions prepared by spray drying method*. Journal of Pharmaceutical Investigation, 2013. **43**(3): p. 205-13.
11. Dong, J., et al., *Intra-articular delivery of liposomal celecoxib–hyaluronate combination for the treatment of osteoarthritis in rabbit model*. International Journal of Pharmaceutics, 2013. **441**(1–2): p. 285-90.
12. Shaji, J. and Bhatia, V., *Proliposomes: a brief overview of novel delivery system*. International Journal of Pharma and Bio Sciences, 2013. **4**(1): p. 150-60.
13. Zheng, B., et al., *Proliposomes containing a bile salt for oral delivery of Ginkgo biloba extract: Formulation optimization, characterization, oral bioavailability and tissue distribution in rats*. European Journal of Pharmaceutical Sciences, 2015. **77**: p. 254-64.
14. Porter, C.J., Trevaskis, N.L., and Charman, W.N., *Lipids and lipid-based formulations: optimizing the oral delivery of lipophilic drugs*. Nature Review Drug Discovery, 2007. **6**(3): p. 231-48.
15. Torchilin, V.P., *Recent advances with liposomes as pharmaceutical*

- carriers*. Nature Review Drug Discovery, 2005. **4**(2): p. 145-60.
16. Jahn, A., et al., *AAPE proliposomes for topical atopic dermatitis treatment*. Journal of Microencapsulation, 2014. **31**(8): p. 768-73.
 17. Tantisripreecha, C., et al., *Development of delayed-release proliposomes tablets for oral protein drug delivery*. Drug Development and Industrial Pharmacy, 2012. **38**(6): p. 718-27.
 18. Yan-yu, X., et al., *Preparation of silymarin proliposome: A new way to increase oral bioavailability of silymarin in beagle dogs*. International Journal of Pharmaceutics, 2006. **319**(1-2): p. 162-8.
 19. Elhissi, A.M.A. and Taylor, K.M.G., *Delivery of liposomes generated from proliposomes using air-jet, ultrasonic, and vibrating-mesh nebulisers*. Journal of Drug Delivery Science and Technology, 2005. **15**(4): p. 261-5.
 20. Gala, R.P., et al., *A comprehensive production method of self-cryoprotected nano-liposome powders*. International Journal of Pharmaceutics, 2015. **486**(1-2): p. 153-8.
 21. Liu, G., et al., *Preparation of 10-hydroxycamptothecin proliposomes by the supercritical CO₂ anti-solvent process*. Chemical Engineering Journal, 2014. **243**: p. 289-96.
 22. Kim, J.E., et al., *Pharmacokinetic properties and bioequivalence of 2 formulations of valsartan 160-mg tablets: A randomized, single-dose, 2-period crossover study in healthy Korean male volunteers*. Clinical Therapeutics, 2014. **36**(2): p. 273-9.
 23. Elhissi, A.M.A., et al., *A study of size, microscopic morphology, and dispersion mechanism of structures generated on hydration of*

- proliposomes*. Journal of Dispersion Science and Technology, 2012. **33**(8): p. 1121-6.
24. Wu, G., et al., *Interaction between Lipid Monolayers and Poloxamer 188: An X-Ray Reflectivity and Diffraction Study*. Biophysical Journal, 2005. **89**(5): p. 3159-73.
25. Bohr, A., et al., *Preparation of microspheres containing low solubility drug compound by electrohydrodynamic spraying*. International Journal of Pharmaceutics, 2011. **412**(1-2): p. 59-67.
26. Chavan, R.B., Modi, S.R., and Bansal, A.K., *Role of solid carriers in pharmaceutical performance of solid supersaturable SEDDS of celecoxib*. International Journal of Pharmaceutics, 2015. **495**(1): p. 374-84.
27. Mathlouthi, M., Benmessaoud, G., and Rogé, B., *Role of water in the polymorphic transitions of small carbohydrates*. Food Chemistry, 2012. **132**(4): p. 1630-7.
28. Kim, E.J., et al., *Preparation of a solid dispersion of felodipine using a solvent wetting method*. European Journal of Pharmaceutics and Biopharmaceutics, 2006. **64**(2): p. 200-5.
29. Zhao, P., et al., *Inclusion of celecoxib into fibrous ordered mesoporous carbon for enhanced oral bioavailability and reduced gastric irritancy*. European Journal of Pharmaceutical Sciences, 2012. **45**(5): p. 639-47.
30. Tayel, S.A., et al., *Duodenum-triggered delivery of pravastatin sodium via enteric surface-coated nanovesicular spanlastic dispersions: development, characterization and pharmacokinetic assessments*. International Journal of Pharmaceutics, 2015. **483**(1-2): p. 77-88.

31. Freitas, C. and Müller, R.H., *Effect of light and temperature on zeta potential and physical stability in solid lipid nanoparticle (SLN™) dispersions*. International Journal of Pharmaceutics, 1998. **168**(2): p. 221-9.
32. Flesch, G., Muller, P., and Lloyd, P., *Absolute bioavailability and pharmacokinetics of valsartan, an angiotensin II receptor antagonist, in man*. European Journal of Clinical Pharmacology, 1997. **52**(2): p. 115-20.
33. Chawla, G., et al., *Characterization of solid-state forms of celecoxib*. European Journal of Pharmaceutical Sciences, 2003. **20**(3): p. 305-17.
34. Zhao, N. and Augsburger, L.L., *The influence of swelling capacity of superdisintegrants in different pH media on the dissolution of hydrochlorothiazide from directly compressed tablets*. AAPS PharmSciTech, 2005. **6**(1): p. E120-6.
35. Hauss, D.J., *Oral lipid-based formulations*. Advanced Drug Delivery Reviews, 2007. **59**(7): p. 667-76.
36. Paulson, S.K., et al., *Pharmacokinetics of celecoxib after oral administration in dogs and humans: effect of food and site of absorption*. Journal of pharmacology and experimental therapeutics, 2001. **297**(2): p. 638-45.

Table 1

Composition of the developed proliposomal formulations.

Component	Blank PLs	VSTPLs	CXBPLs
SPC	20.0% (800 mg)	19.2% (800 mg)	19.5% (800 mg)
Sorbitol	79.0% (3160 mg)	76.0% (3160 mg)	77.1% (3160 mg)
Poloxamer 188	1.0% (40 mg)	1.0% (40 mg)	1.0% (40 mg)
VST	-	3.8% (160 mg)	-
CXB	-	-	2.4% (100 mg)
Total	100% (4000 mg)	100% (4160 mg)	100% (4100 mg)

Table 2

Characterization of the developed proliposomal formulations.

Formulation	Mean diameter (nm)	Polydispersity index	Zeta potential (mV)	Entrapment efficiency (%) ^a	Drug content (%) ^b
Blank PLs	365.6 ± 14.5	0.30 ± 0.02	-59.00 ± 0.09	-	-
VSTPLs	368.8 ± 30.7	0.29 ± 0.08	-57.42 ± 0.36	77.5 ± 2.8	3.71 ± 0.04
CXBPLs	537.1 ± 10.2	0.36 ± 0.01	-64.15 ± 0.26	84.7 ± 1.2	2.35 ± 0.09

$$^a\text{Entrapment efficiency (\%)} = \frac{\text{actual drug amount in liposomal dispersion after filtration}}{\text{theoretical drug amount in liposomal dispersion}} \times 100$$

$$^b\text{Drug content (\%)} = \frac{\text{actual drug amount in proliposomes}}{\text{total weight of proliposomes}} \times 100$$

Data are presented as mean ± SD ($n = 3$).

Table 3

Pharmacokinetic parameters of VST after oral administration of crude VST powder and VSTPLs at a dose of 3 mg/kg in rats.

Parameter	crude VST powder	VSTPLs
AUC ($\mu\text{g}\cdot\text{min}/\text{mL}$)	160 \pm 50	291 \pm 72*
C _{max} ($\mu\text{g}/\text{mL}$)	0.70 \pm 0.25	1.32 \pm 0.30*
T _{max} (min)	45 \pm 15	58 \pm 29
Relative bioavailability (%)	100	182

* $p < 0.05$, compared to crude VST powder group.

Data are presented as mean \pm SD ($n \geq 3$).

Table 4

Pharmacokinetic parameters of CXB after oral administration of crude CXB powder, Celebrex, and CXBPLs at a dose of 2 mg/kg in rats.

Parameter	crude CXB powder	Celebrex	CXBPLs
AUC ($\mu\text{g}\cdot\text{min}/\text{mL}$)	464 \pm 117	774 \pm 165*	803 \pm 139*
C _{max} ($\mu\text{g}/\text{mL}$)	0.56 \pm 0.17	1.05 \pm 0.44	1.12 \pm 0.23*
T _{max} (min)	240 \pm 0	165 \pm 90	64 \pm 19*
Relative bioavailability (%)	100	167	173

* $p < 0.05$, compared to crude CXB powder group.

Data are presented as mean \pm SD ($n \geq 3$).

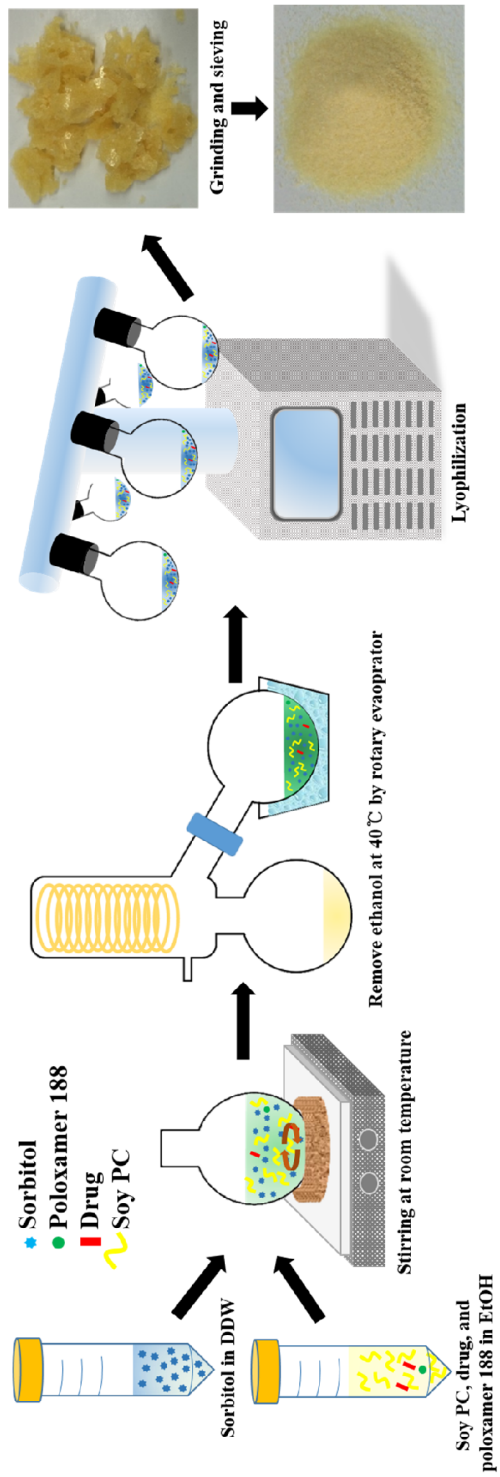


Figure 1. Schematic illustration of the preparation method of PLs.

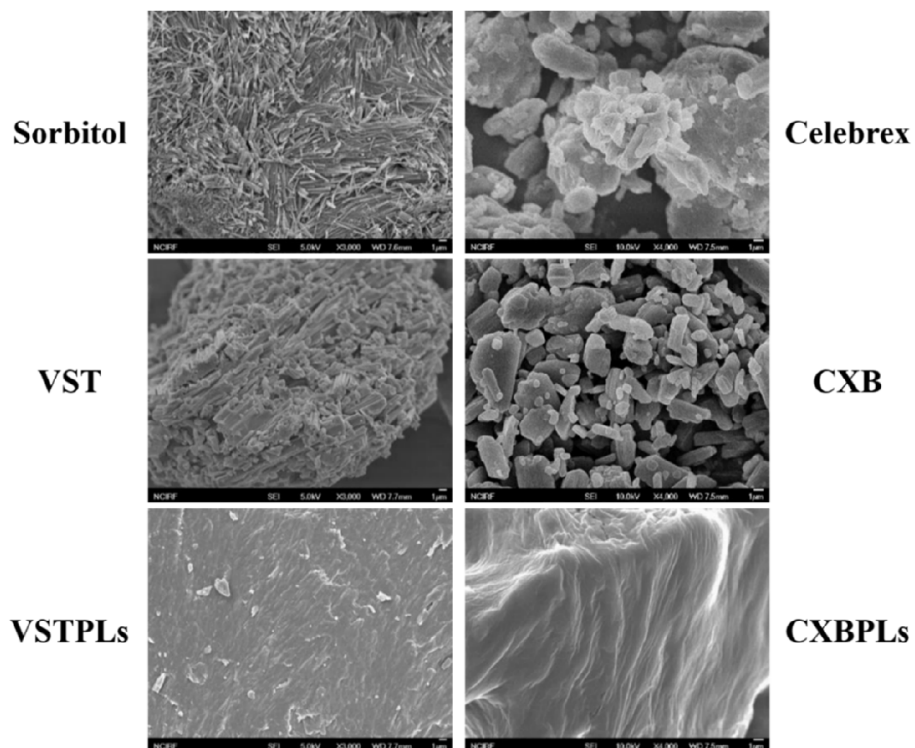


Figure 2. SEM images of sorbitol, VST, CXB, Celebrex, VSTPLs, and CXBPLs. The lengths of the scale bars are 1 μm .

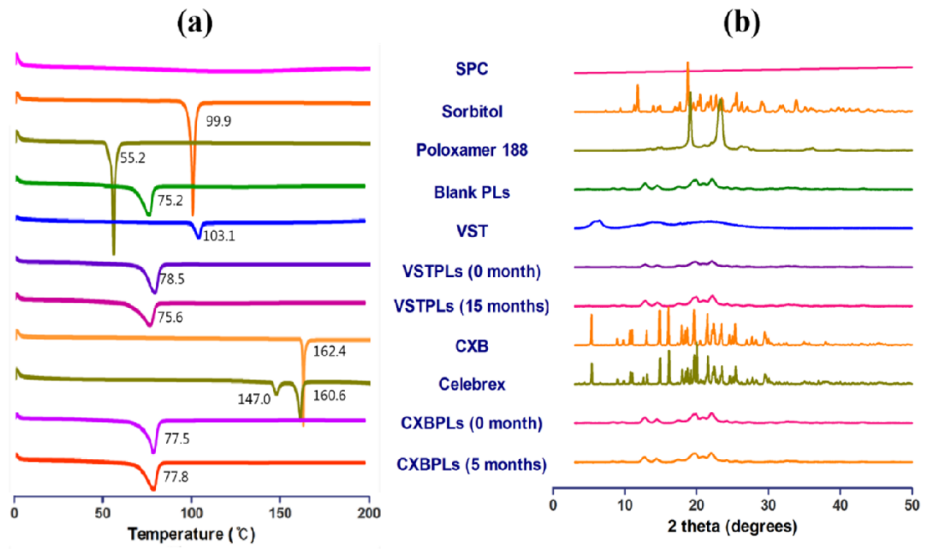


Figure 3. Characterization of VSTPLs and CXBPLs. (a) DSC thermograms and (b) X-ray diffraction patterns.

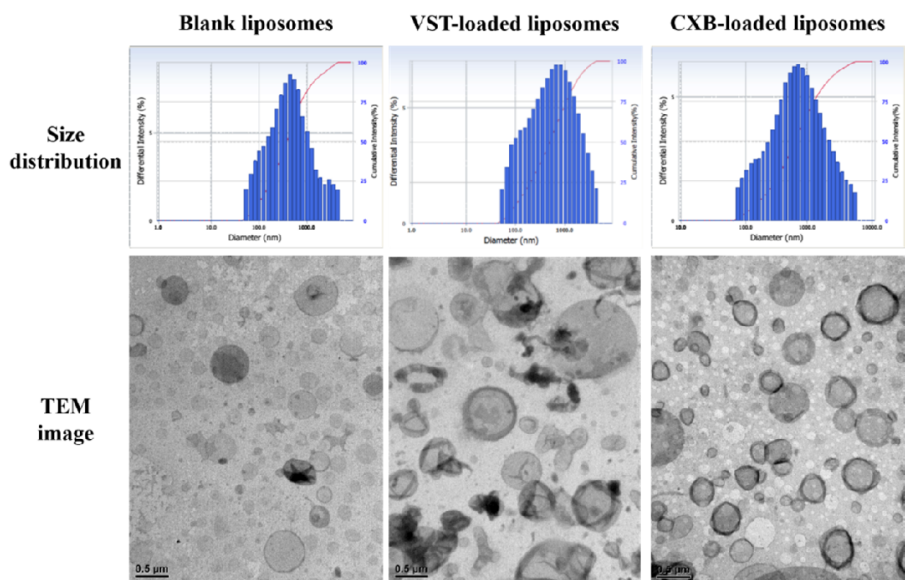


Figure 4. Size distribution and TEM images of the liposomes after reconstitution of blank PLs, VSTPLs, and CXBPLs. The length of the scale bars are 0.5 μm .

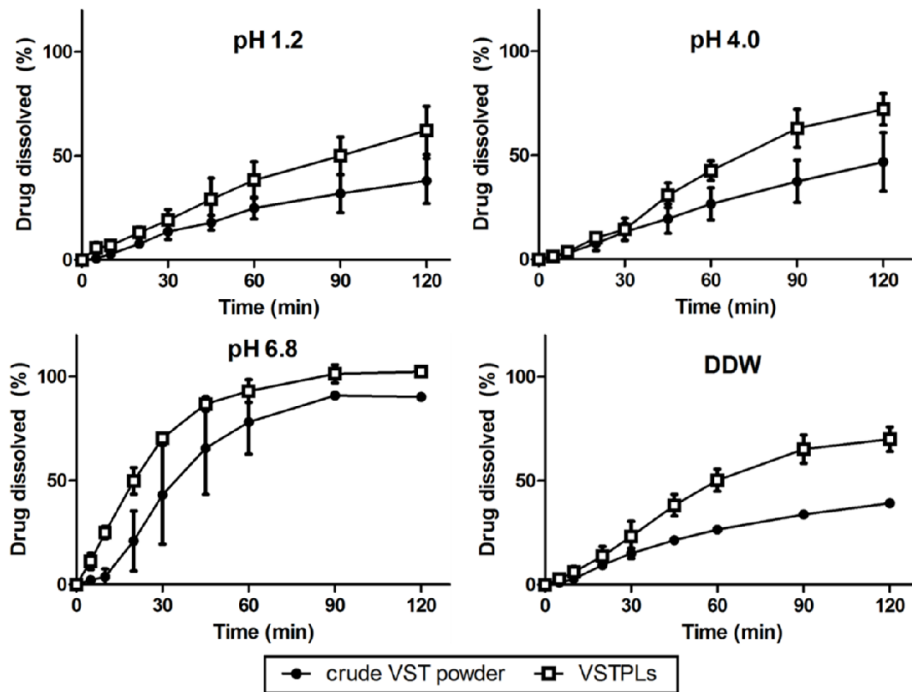


Figure 5. *In vitro* dissolution profiles of crude VST powder and VSTPLs at pH 1.2, 4.0, 6.8, and DDW. Data are presented as the mean \pm SD ($n = 3$).

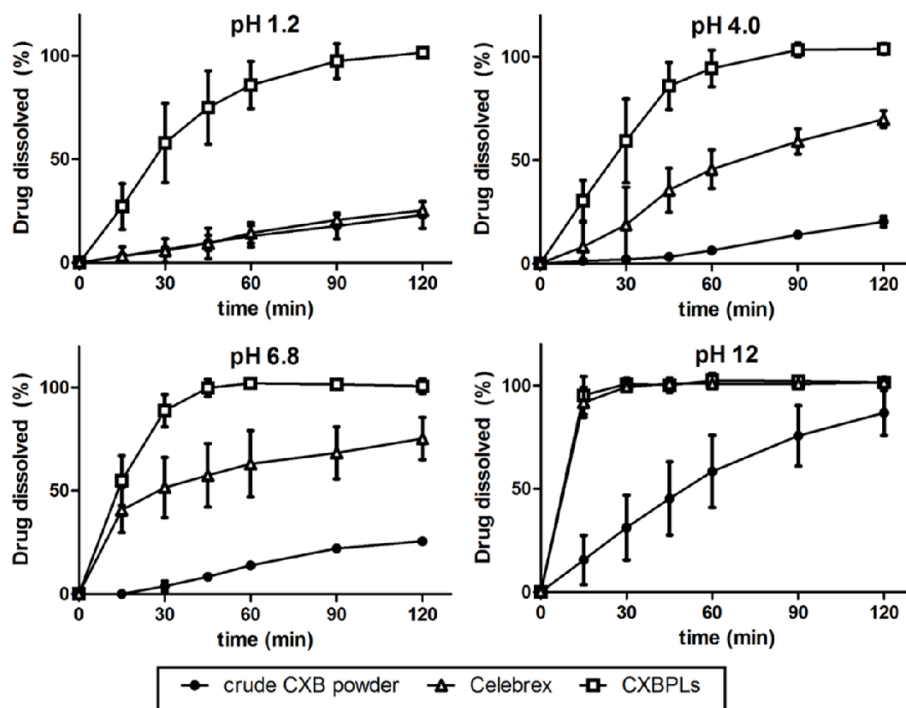


Figure 6. *In vitro* dissolution profiles of crude CXB powder, Celebrex, and CXBPLs at pH 1.2, 4.0, 6.8, and 12.0. Data are presented as the mean \pm SD ($n = 3$).

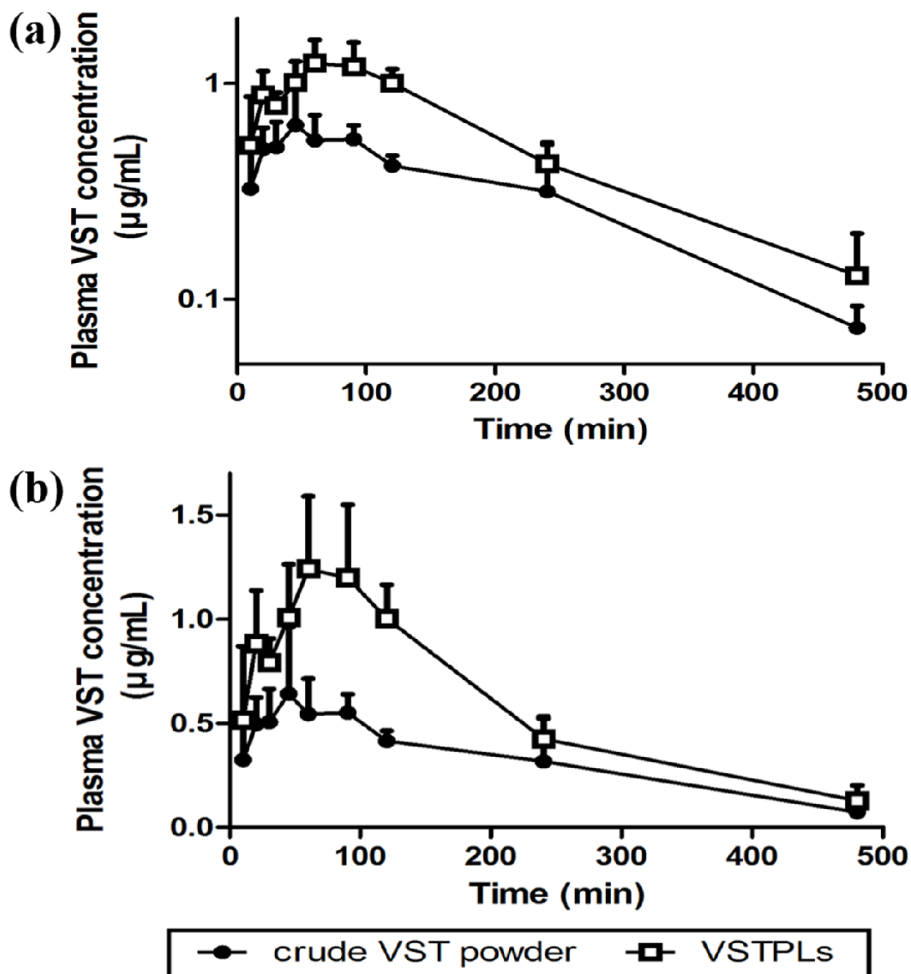


Figure 7. Plasma concentration vs. time profiles of VST after a single oral administration of crude VST powder and VSTPLs at a dose of 3 mg/kg. The values are presented on a (a) semilogarithmic plot and (b) linear scale. Data are presented as the mean \pm SD ($n \geq 3$).

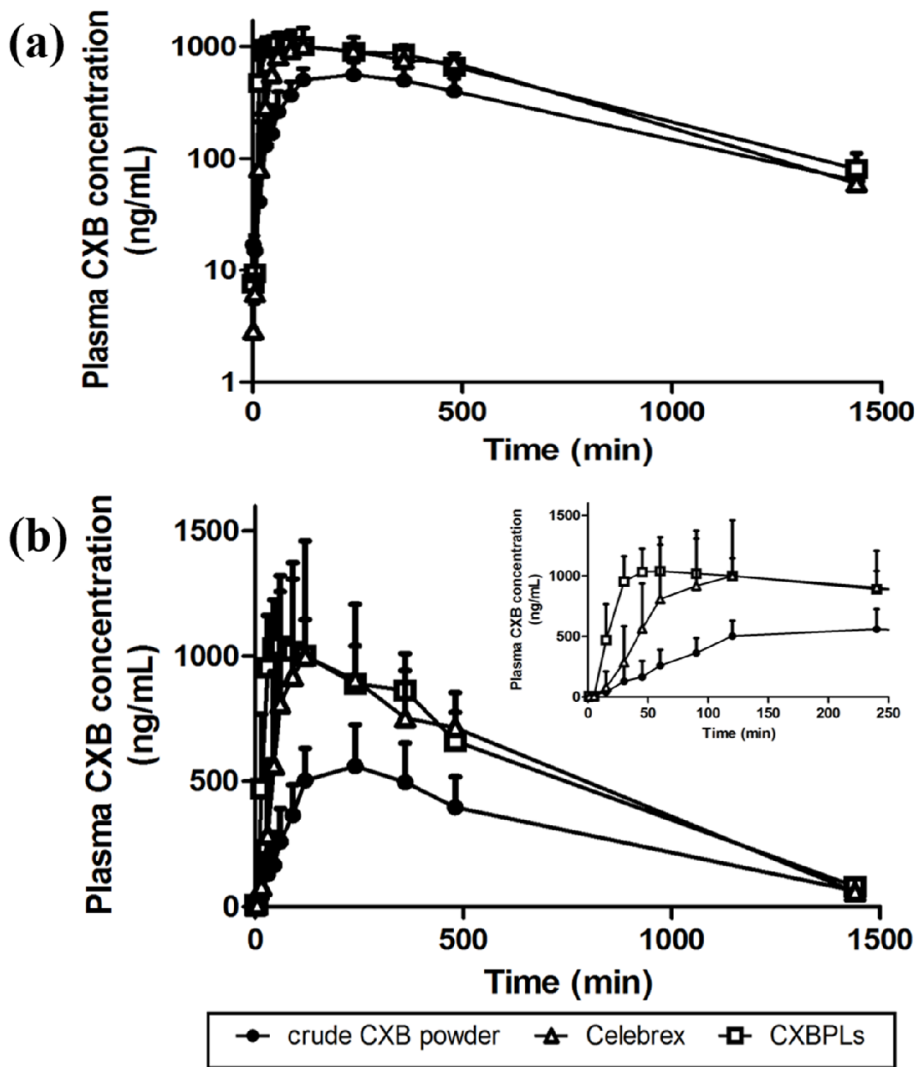


Figure 8. Plasma concentration vs. time profiles of CXB after a single oral administration of crude CXB powder, Celebrex, and CXBPLs at a dose of 2 mg/kg. The values are presented on a (a) semilogarithmic plot and (b) linear scale (inset: expanded view from time 0 to 250 min). Data are presented as the mean \pm SD ($n \geq 3$).

Supplementary Information

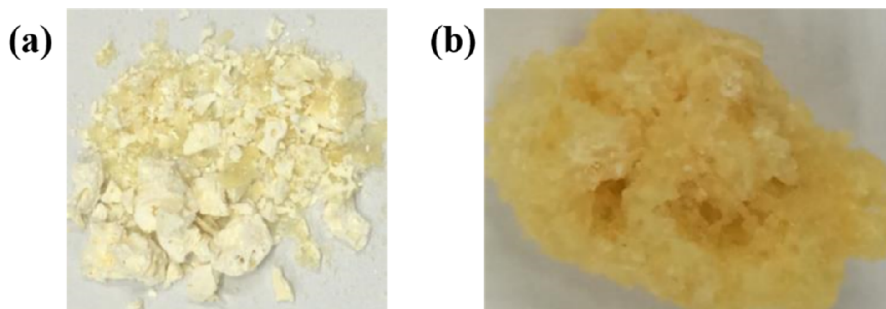


Figure S1. Images of PLs prepared (a) without solvent evaporation step and (b) with the 25% (w/w) of lipid content.

The solvent evaporation of ethanol before lyophilization is a critical step for homogeneous formulation. As mentioned in 3.1, without removal of ethanol, phase separation occur during lyophilization, since the tripe point of ethanol is too low to sublime by lyophilization. Ethanol in the solution melt down and withdraw ethanol-soluble material such as drugs and SPC from the solution during lyophilization process. This result in inhomogeneous formulation (Figure S1a).

To increase the amount of reconstituted liposomes in unit weight of the proliposomal formulation, a high lipid to matrix ratio of PLs is desirable. However, when the lipid content of PLs was over 20% (w/w), the stickiness of lipid remained in prepared PLs which made it difficult to modify further (Figure S1b).

Table S1

Composition and evaporation temperature of simvastatin-loaded proliposomes (SVPLs)

Component	SVPL - 60°C	SVPL - 40°C
SPC	19.2% (800 mg)	19.2% (800 mg)
Sorbitol	76.0% (3160 mg)	76.0% (3160 mg)
Poloxamer 188	1.0% (40 mg)	1.0% (40 mg)
SV	3.8% (160 mg)	3.8% (160 mg)
Evaporation temperature	60°C	40°C

Table S2

Characterization of SVPLs.

Formulation	Batch No.	Mean diameter (nm)	Polydispersity index	Entrapment efficiency (%)^a
SVPL - 60°C	1	598.8 ± 20.9	0.33 ± 0.05	73.0 ± 11.6
	2	925.6 ± 62.1	0.36 ± 0.02	33.0 ± 5.8
	3	768.7 ± 9.9	0.31 ± 0.00	51.7 ± 4.2
SVPL - 40°C	1	615.8 ± 11.7	0.35 ± 0.00	72.4 ± 1.8
	2	584.4 ± 29.6	0.35 ± 0.03	71.2 ± 3.2
	3	570.3 ± 45.9	0.34 ± 0.06	72.8 ± 3.7

$$^a\text{Entrapment efficiency (\%)} = \frac{\text{actual drug amount in liposomal dispersion after filtration}}{\text{theoretical drug amount in liposomal dispersion}} \times 100$$

Data are presented as mean ± standard deviation (SD) ($n = 3$).

Optimization of the temperature of solvent evaporation was conducted using simvastatin (SV) as model drug in the preliminary study. Preparation of SV-loaded proliposomes (SVPLs) was conducted at high (60°C) and low (40°C) temperature

of solvent evaporation (Table S1). The particle size and EE of reconstituted SV-loaded liposomes were evaluated (Table S2).

To determine SV concentration, reverse-phase HPLC was performed on a Waters e1515 system consisting of a 2487 dual λ absorbance detector (Waters Corporation, USA). For the chromatographic separation of SV, a Phenomenex Gemini-NX analytical column (250×4.6 mm, $5 \mu\text{m}$) was used. The wavelength for detection was set at 238 nm. The determination was carried out by isocratic elution using ACN / 20 mM phosphate buffer (pH 5.6) (80:20, v/v) mixture as the mobile phase at a flow rate of 1.0 mL/min. All samples were appropriately diluted with mobile phase prior to analysis.

The particle size and EE were variable among batches when the solvent evaporation conducted at high temperature (60°C). Meanwhile, the particle size and EE were even among batches when evaporation processed at low temperature (40°C). This might be resulted from the volume of solution before lyophilization. At 60°C , due to not only ethanol but also DDW was evaporated in rotary evaporator, the final volume of solution was different among batches, caused variability. However, at 40°C , DDW could not evaporated in rotary evaporator, the final volume before lyophilization was relatively consistent among batches, result in uniformity. Therefore, the evaporation condition was set to 40°C .

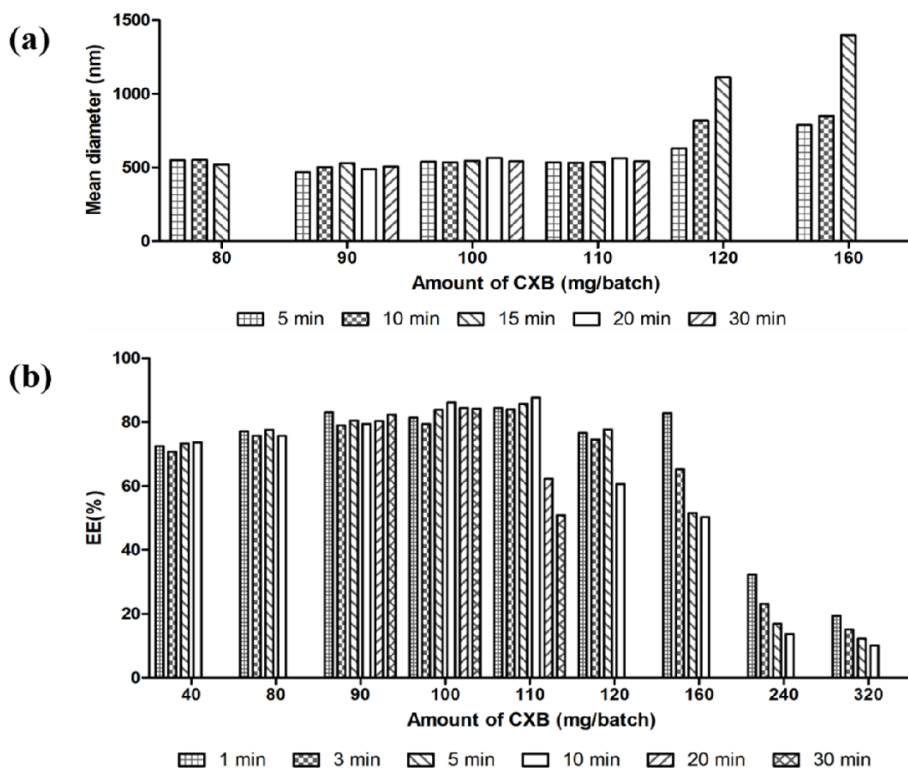


Figure S2. The effect of the amount of CXB in CXBPLs on the (a) mean diameter and (b) EE values after reconstitution.

The amount of CXB in CXBPLs was determined based on the mean diameter and EE of reconstituted CXB-loaded liposomes. As shown in Figure S2a, only the CXBPL batches with not more than 110 mg of CXB maintained their mean diameter for 30 min after reconstitution. Similarly, the CXBPL batches with not more than 100 mg of CXB maintained CXB-loaded liposomes (Figure S2b). The CXBPL batches with more than 110 mg of CXB showed CXB precipitation with time. Therefore, the amount of CXB in a batch of CXBPLs was set at 100 mg (Table 1).

Table S3

Solubility of VST in various media.

pH of buffer	pH 1.2	pH 4.0	pH 6.8	DDW
Solubility ($\mu\text{g/mL}$)	58.73 ± 0.98	272.19 ± 2.30	3108.96 ± 14.32	143.17 ± 1.07

Data are presented as mean \pm standard deviation (SD) ($n = 3$).

The solubility of VST at various pH was used to determine sink condition of *in vitro* dissolution studies (Table S2). Approximately 10 to 50 mg of VST was dispersed in 15mL of media at various pH (pH 1.2, 4.0, 6.8, and DDW) and vortexed for 30 min. Then, the tubes were incubated in a shaking water bath operated at 50 rpm at 37 °C. After 48 h incubation, the tubes were centrifuged at 3,000 rpm for 15 min (MF80, Hanil Science, Korea). An aliquot (1.4 mL) of supernatant was transferred to eppendorf tube and centrifuged at 13,200 rpm for 15 min (5415R, Eppendorf centrifuge, Germany). An aliquot (1 mL) of supernatant was filtered through a 0.2 μm syringe filter (Minisart RC15, Sartorius, Germany), and properly diluted prior to measuring the drug concentration by means of HPLC in the section 2.3.2.3. The volume of dissolution media for the study was chosen at 500 mL, except for pH 1.2 buffer at 1,000 mL to satisfy the sink condition according to 'USP 38 General

Information <1092> The Dissolution Procedure'.

Table S4

Solubility of CXB in various media.

% of SDS (w/v)	CXB solubility ($\mu\text{g/mL}$)				
	pH 1.2	pH 4.0	pH 6.8	pH 12.0	DDW
0.0	1.41 \pm 0.03	1.55 \pm 0.07	1.23 \pm 0.05	312.46 \pm 25.18	2.06 \pm 0.10
0.1	26.04 \pm 2.13	4.38 \pm 0.52	9.41 \pm 0.59	485.11 \pm 31.55	2.52 \pm 0.20
0.4	168.91 \pm 3.12	198.17 \pm 2.02	161.92 \pm 7.88	1168.53 \pm 33.21	129.86 \pm 4.74
0.7	289.23 \pm 5.52	385.12 \pm 5.45	331.54 \pm 10.59	1670.34 \pm 17.65	344.05 \pm 2.40
1.0	420.42 \pm 5.86	580.40 \pm 3.81	512.46 \pm 7.95	2271.35 \pm 41.36	545.56 \pm 14.21

Data are presented as mean \pm standard deviation (SD) ($n = 3$).

The solubility of CXB at various pH with various SDS concentration was evaluated to determine sink condition of *in vitro* dissolution studies (Table S3). The aqueous solubility of CXB was determined in various pH (pH 1.2, 4.0, 6.8, 12.0, and DDW) with 0.1%, 0.4%, 0.7%, and 1.0% (w/v) SDS. Approximately 3 mg of CXB was dispersed in 1.5 mL media and vortex-mixed for 30 min. Then, the tubes were incubated in a shaking water bath operated at 50 rpm at 37°C. After 48 h incubation, the tubes

were centrifuged at 13,200 rpm for 15 min, an aliquot (1 mL) of supernatant was filtered through a 0.2 µm syringe filter (Minisart RC15, Sartorius, Germany), and properly diluted prior to HPLC analysis as described at 2.3.2.3 section. The 500 mL of media with 0.4% (w/v) SDS was chosen for the dissolution tests.

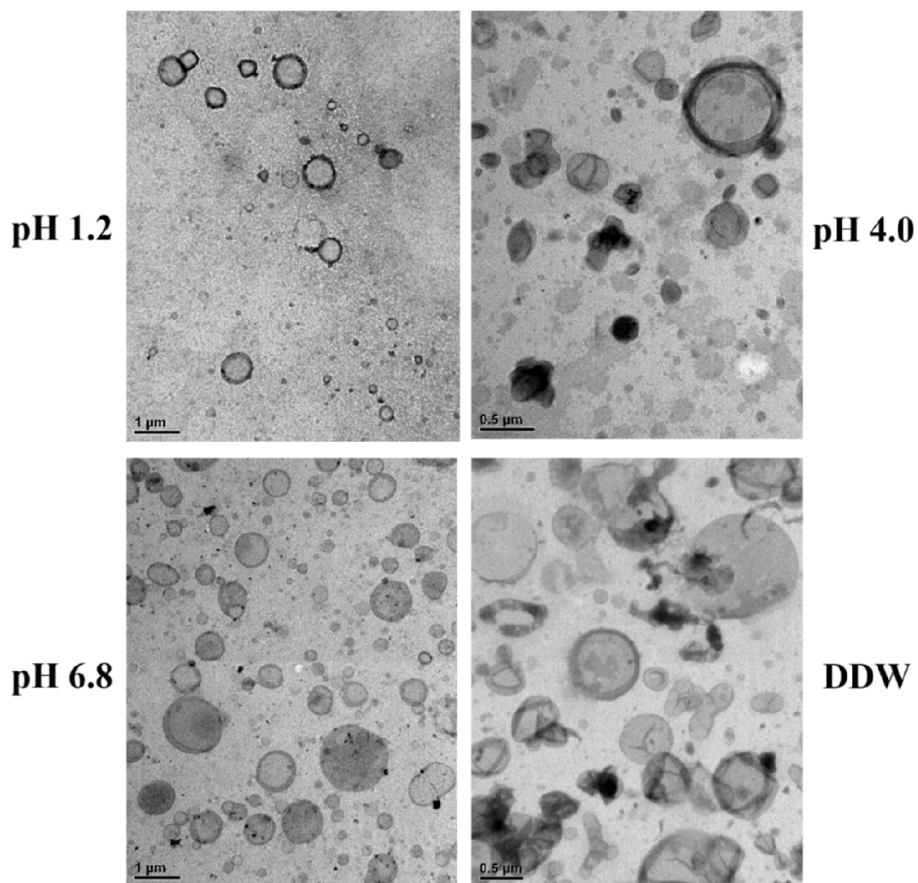


Figure S3. TEM images of VST-loaded liposomes in various dissolution media (pH 1.2, 4.0, 6.8, and DDW). The length of the scale bars are shown in Figure.

The reconstitution of VST-loaded liposomes from VSTPLs in various dissolution media (pH 1.2, 4.0, 6.8, and DDW) were observed by TEM as described in 2.3.2.1. Spherical liposomes were form in all dissolution media. The formation of liposomes could attribute to improve dissolution of VST of VSTPLs (Figure 5).

국문초록

향상된 경구 생체이용률을 위한 BCS

class II 약물의 프로리포솜 적용:

발사르탄과 세레콕시브

Purpose. 본 연구의 목적은 기존 제법보다 간편하면서도 높은 지질 함량을 갖는 프로리포솜 (Proliposomes, PLs) 제법을 개발하고, BCS class II 모델 약물로 발사르탄 (Valsartan, VST) 과 세레콕시브 (Celecoxib, CXB) 를 첨가한 프로리포솜을 제조 및 평가하는 것이다.

Methods. 회전 증발 응축기와 동결건조기를 사용하여 발사르탄이 봉입된 프로리포솜 (VSTPLs) 과 세레콕시브가 봉입된 프로리포솜 (CXBPLs) 을 제조하였다. 프로리포솜 제조에는 인체에 무독성한 원료 및 용매를 사용하여, 경구투여가 가능하게 하였다. 프로리포솜 내 최고 지질 비율을 확인하고 이를 바탕으로 VSTPLs와 CXBPLs의 조성을 설정하였다. 만들어진 프로리포솜은 주사 전자 현미경 (Scanning electron microscopy, SEM), X-선 회절계 (Powder X-ray diffractometer, PXRD), 시차 주사 열량측정계 (Differential scanning calorimetry, DSC)을 이용하여

고체 상태에서 평가하였다. 프로리포솜을 물에 풀어 재건한 리포솜 (liposomes) 의 입자도, 제타전위, 약물 봉입률 등을 평가하였고, 입자 성상은 투과전자현미경 (Transmission electron microscopy, TEM) 으로 확인하였다. 생체 외 (*in vitro*) 용출 및 랫에서의 생체 내 (*in vivo*) 약물동력학적 평가를 진행하였다.

Results. 상기 제법으로 프로리포솜 내의 지질 비율을 20% (w/w) 까지 증가시킬 수 있었다. 프로리포솜 내 약물은 결정형에서 무정형으로 변형되었다. 재건한 리포솜의 평균 입자경, 제타전위와 약물 봉입률은 VSTPLs에서 각각 369 ± 31 nm, -57.4 ± 0.4 mV, $77.5 \pm 2.8\%$ 이었으며, CXBPLs에서는 각각 537 ± 10 nm, -64.2 ± 0.3 mV, $84.7 \pm 1.2\%$ 이었다. 다양한 pH 환경에서 실시한 약물의 생체 외 (*in vitro*) 용출 평가에서는 프로리포솜 내의 약물이 원료 약물보다 더 빠르고 높은 용출을 보였다. 약물의 생체 내 (*in vivo*) 약물동력학 평가에서 프로리포솜이 원료 약물보다 더 높은 C_{max} 와 AUC 를 보였다.

Conclusions. 상기 제법으로 제조된 프로리포솜은 다음과 같은 장점을 지닌다. (a) 기존 제법보다 쉽고 공정 제어가 간단하며, (b) 사용된 원료와 용매가 무독성이며, (c) 만들어진 프로리포솜은 지질 비율이 높아 많은 양의 수불용성 약물을 봉입할 수 있으며, (d) 프로리포솜 내의 무정형으로 존재하는 약물과, 수상에서 빠르게 형성된 리포솜이 용출을 증가시키고 약물의 경구 생체이용률을 증가시키는 데에 기여한다.

주요어: Proliposomes, Valsartan, Celecoxib, Dissolution rate,
Oral bioavailability

학번: 2014-21972